

The University of Bradford Institutional Repository

<http://bradscholars.brad.ac.uk>

This work is made available online in accordance with publisher policies. Please refer to the repository record for this item and our Policy Document available from the repository home page for further information.

To see the final version of this work please visit the publisher's website. Available access to the published online version may require a subscription.

Link to publisher's version: <https://doi.org/10.1680/jgein.17.00033>

Citation: Mirzababaei M, Mohamed MHA, Arulrajah A, Horpibulsuk S and Anggraini V (2018) Practical approach to predict the shear strength of fibre-reinforced clay. *Geosynthetics International*. 25(1): 50–66.

Copyright statement: © 2018 ICE. Reproduced in accordance with the publisher's self-archiving policy.

Practical approach to predict the shear strength of fibre-reinforced clay

Mehdi Mirzababaei, B.Eng., MSc., PhD (Corresponding author)

Lecturer, School of Engineering and Technology

Central Queensland University, 120 Spencer Street, Melbourne, Victoria 3000, Australia

Email: m.mirzababaei@cqu.edu.au

Tel: +61 3 9610626

Mostafa Mohamed, B.Eng., MSc., PhD

Senior Lecturer, University of Bradford, Faculty of Engineering and Informatics, Bradford, BD7 1DP, the UK

Email: m.h.a.mohamed@bradford.ac.uk

Arul Arulrajah, BSc, MEngSc, PhD

Professor, Department of Civil and Construction Engineering

Swinburne University of Technology, Hawthorn, Victoria 3122, Australia

Email: arulrajah@swin.edu.au

Suksun Horpibulsuk, Professor and Chair, School of Civil Engineering,

Director, Centre for Innovation in Sustainable Infrastructure Development,

Suranaree University of Technology, Nakhon Ratchasima 30000, Thailand

Email: suksun@g.sut.ac.th

Vivi Anggraini, B.Eng., M.Eng. Ph.D

Lecturer, School of Engineering, Monash University Malaysia

Jalan Lagoon Selatan, 47500 Bandar Sunway, Selangor Darul Ehsan, Malaysia

Email: vivi.anggraini@monash.edu

Total number of words (main text excluding abstract and refs): 5643

Number of Figures: 19

Number of Tables: 3

Abstract

Carpet waste fibres have a higher volume to weight ratios and once discarded into landfills, these fibres occupy a larger volume than other materials of similar weight. This research evaluates the efficiency of two types of carpet waste fibre as sustainable soil reinforcing materials to improve the shear strength of clay. A series of consolidated undrained (CU) triaxial compression tests were carried out to study the shear strength of reinforced clays with 1%, to 5% carpet waste fibres. The results indicated that carpet waste fibres improve the effective shear stress ratio and deviator stress of the host soil significantly. Addition of 1%, 3% and 5% carpet fibres could improve the effective stress ratio of the unreinforced soil by 17.6%, 53.5% and 70.6%, respectively at an initial effective consolidation stress of 200 kPa. In this study, a nonlinear regression model was developed based on a modified form of the hyperbolic model to predict the relationship between effective shear stress ratio, deviator stress and axial strain of fibre-reinforced soil samples with various fibre contents when subjected to various initial effective consolidation stresses. The proposed model was validated using the published experimental data, with predictions using this model found to be in excellent agreement.

Key words: Geosynthetics, Shear strength, Carpet waste fibre, Reinforced soil, Clays, Modified hyperbolic model

Notations:

Basic SI units are shown in parentheses.

q_{ratio}	deviator stress ratio (dimensionless)
p'_{ratio}	average mean effective stress ratio (dimensionless)
q	deviator stress (Pa)
p'	mean effective stress (Pa)
q_{re}	deviator stress of fibre-reinforced soil (Pa)
q_{un}	deviator stress of unreinforced soil (Pa)
$(\frac{q}{p'})_{re}$	effective stress ratio of fibre-reinforced soil (dimensionless)
$(\frac{q}{p'})_{un}$	effective stress ratio of unreinforced soil (dimensionless)
p'_{re}	mean effective stress of fibre-reinforced soil (Pa)
p'_{un}	mean effective stress of unreinforced soil (Pa)
σ'_1	major principal effective stress (Pa)
σ'_3	minor principal effective stress (Pa)
z, w	coefficients of the linear relationship between q_{ratio} and p'_{ratio} (dimensionless)
ε	axial strain in triaxial shear test (dimensionless)
a, b, n, g, h, t	modified hyperbolic model parameters (dimensionless)
$a^*, b^*, n^*, g^*, h^*, t^*$	normalised modified hyperbolic model parameters (dimensionless)
σ'_c	initial effective consolidation stress (Pa)
f	fibre content (dimensionless)
$k_{1a,g}, k_{2a,g}, k_{1b,h}, k_{2b,h}, k_{1n,t}, k_{2n,t}$	coefficients of the linear equations for normalised model parameters (dimensionless)

1. Introduction

The carpet manufacturing industry produces a large quantity of fibre wastes due to aspects such as the end of line leftovers, stop-start wastage, yarn breakages, faults and quality control. In addition, as the demand for new carpets increases, substantial amounts of old and post-consumer carpet wastes have to be disposed to landfills. Synthetic fibres used in carpet manufacturing are particularly problematic as they do not degrade with time and once dumped into landfills, may release colour pigments in the surrounding soil. This may pollute the underground water reservoirs, which are potential sources for domestic use. Local communities, businesses and governmental agencies are increasingly encouraged to re-use and recycle carpet waste fibres, so as to minimise the need for landfilling. Virgin discrete synthetic/natural fibres have been used in geotechnical engineering practice to improve the stress-strain response of fine and coarse-grained soils. Upon mixing with soil particles, short discrete fibres behave like tension resisting elements interlocking soil particles to partially withstand shear stresses within the soil. This results in the formation of a composite coherent soil matrix that possesses superior strength properties with reduced and/or eliminated continuous planes of weakness at failure (Ahmad et al., 2010). The reinforcing role of short virgin synthetic fibres in coarse-grained soils with loose to dense states has been studied previously (Maher and Gray 1990; Nataraj 1997; Consoli et al. 2007; Diambra et al. 2007, 2010; Chen and Loehr 2009; Hamidi and Hooresfand 2013; Miranda Pino et al. 2015; and Jamsawang et al. 2015). The behaviour of fibre-reinforced fine-grained soils has also been studied previously (Falorca et al. 2006; Casagrande et al. 2006; Özkul and Baykal 2007; Al-Akhras et al. 2010; Babu and Chouksey 2010; Ekinici and Ferreira 2012; Maliakal and Thiyyakkandi 2013; Sadeghi and Beigi 2014 and Botero et al. 2015; Khatri et al. 2015; and Anggraini et al. 2016). The reported research findings are in agreement in that fibre reinforcement improves the stress-strain behaviour, unconfined compression strength, shear strength and ductility of the soil and reduces the consolidation settlement of clay. Currently, the research theme within the area of soil fibre reinforcement is strongly favoured towards the use of virgin short fibres, mostly with granular soils. There is presently a research gap on the utilisation of recycled carpet waste fibres for the reinforcement of clays, with only limited current publications on this aspect (Murray et al. 2000, Ghiassian et al. 2004, Fatahi et al. 2012, 2013 a & b and Mirzababaei et al. 2013 a & b, 2017 b).

Murray et al. (2000) conducted a consolidated undrained compression triaxial testing program to investigate the shear strength of a reinforced sandy silt soil with nylon waste fibres and virgin fibrillated polypropylene fibres. The results indicated that adding up to 3% waste nylon fibre or a maximum of 1% polypropylene virgin fibre can significantly increase the peak shear strength of the soil and can reduce its post-peak reduction in a ductile manner. Based on a series of drained compression triaxial tests on sand samples reinforced with carpet waste strips, Ghiassian et al. (2004) reported a satisfactory degree of improvement in the peak shear strength of sand that could be achieved by either increasing the strip content at a constant aspect ratio or by increasing the aspect ratio at a constant strip content.

Recently, Fatahi et al. (2012, 2013 b) reported the improving effect of carpet waste fibre addition to cement stabilised soft kaolin and stated that the fibre type and content could significantly influence the peak shear strength,

stiffness and brittleness of the soft clays. The initial Young's modulus of the cement-stabilised clay increased with the addition of polypropylene fibres, but reduced with the addition of carpet and steel fibres.

Mirzababaei et al. (2013 a and b) carried out an extensive testing programme to investigate the unconfined compression strength and swelling pressure of expansive clays reinforced with carpet waste fibres and concluded that inclusion of up to 5% carpet waste fibres could result in reduction of the swelling pressure and increasing the unconfined compression strength of the clay. However, the relative gain in unconfined compression strength and reduction in swelling pressure is highly dependent on the initial dry unit weight and the moisture content of the clay. Mirzababaei et al. (2017 b) also reported significant enhancement in the bearing capacity of a model footing on a clay slope reinforced with carpet waste fibre. In this study, the stress-strain behaviour of a clay reinforced with two types of carpet waste fibre was analysed by conducting a number of consolidated undrained triaxial compression tests. Thus the experimental programme in this research seeks to evaluate the feasibility to sustainably reuse carpet waste fibres with non-uniform lengths and thicknesses to enhance the shear strength of clay.

Several analytical models are available to estimate the stress-strain behaviour of fibre-reinforced granular soils based on the force-equilibrium approach (Waldron 1977; Gray and Ohashi 1983; Maher and Gray 1990; Ranjan et al. 1996; Michalowski 2008; Shukla et al. 2010), energy-based model (Michalowski and Zhao 1996) and discrete framework model (Zornberg 2002). There are also several statistical models to predict the shear strength of fibre-reinforced granular soils (Ranjan et al 1996; Babu and Vasudevan 2008) with input parameters including some or any of the following: fibre content, fibre aspect ratio, fibre surface friction, confining pressure, fibre length, cohesion and internal friction angle of the fibre-reinforced soil. Cam Clay constitutive model has also been reformulated to account for the estimation of the deviator stress of fibre-reinforced clays (Chen 2007; Babu and Chouksey 2010; Diambra and Ibraim 2014 and Nguyen and Fatahi 2016).

Although all proposed analytical and constitutive models agree well with the experimental data, the parameters required to execute these models are complex and require a number of triaxial, direct shear and consolidation tests. Therefore, due to the variability of soil types, fibre types and the complex interfacial behaviour of the soil at the interface with fibres, it is required to estimate the shear strength properties of the fibre-reinforced soil with less effort, so as to obtain the soil/fibre input parameters to ease its application in practice. In this study, a simple regression model is developed to predict the relationship between the effective shear strength ratio (q/p'), deviator stress (q) and the axial strain of a fibre-reinforced clay subjected to axial deviator stress at any fibre content and confining pressure regardless the fibre type and clay type.

2. Materials

The soil sample used in this study was collected from a site in the Northwest region of the United Kingdom. The soil was classified as low plastic clay according to the Unified Soil Classification System (USCS) with a plasticity index of 17% and specific gravity of 2.68. The grain size analysis of the soil indicated that it contained 55.78% fine grains and 44.22% coarse grains. **Table 1** shows the properties of the soil. Two different types of carpet waste fibre (i.e., herein called GBF and ABF) were utilised in this investigation and supplied by Carpet Recycling UK and Milliken Carpet Europe as waste by-products from the production line (i.e. from shearing and/or edge trimming of the

carpet). The GBF consisted predominantly of propylene fibres whereas the ABF included short nylon fibres. **Table 2** presents typical specifications of the carpet waste fibres used in this study. Due to the waste origin of the fibres used in this study, the length of the fibres ranged from 2 to 20 mm with diverse thicknesses from 80 μm to 1,500 μm .

3. Experimental Programme

In this study, because carpet fibre is classified as waste material, it was decided to investigate the addition of a high proportion of waste fibres on the shear strength of the clay. Therefore, fibre contents of 1%, 3%, and 5% of the dry mass of soil were selected to reinforce the clay. Because of reduced workability and practical difficulties to mix higher fibre contents evenly with the soil, the maximum fibre content used in this study was limited to 5%. Standard Proctor compaction tests were carried out on the unreinforced and fibre-reinforced clay. The compaction test results revealed that the maximum dry unit weight of the soil decreases with fibre inclusion. **Figure 1** presents the compaction curves of the unreinforced and carpet waste fibre-reinforced soil with both fibre types. To achieve a uniform distribution of fibres in the clay sample, various approaches were undertaken including mixing water soaked fibres with dry clay, addition of dry fibres to the wet clay followed by mixing and mixing dry clay and fibres followed by spraying water on the mixture. It was concluded that spraying water on a dry mixture of fibre and clay to achieve the desired moisture content results in producing relatively uniform samples with less fibre tangling. However, other examined methods led to the formation of fibre lumps or balling during preparation that could affect the homogeneity of the sample. Therefore, the dry soil and fibres were mixed thoroughly in a sealed container by shaking. Subsequently, the calculated amount of water to reach the target moisture content was sprayed over the dry mixture of soil and fibre in several stages, followed by hand mixing to prepare a uniform mixture. The prepared mixture was kept in a sealed container for 3 to 4 days before the test day. This procedure, could possibly increase the mixing efficiency and therefore, ensure a relative uniformity of fibre distribution in the fibre-reinforced soil sample.

A series of consolidated undrained triaxial tests were carried out on unreinforced and fibre-reinforced clay samples following BS 1377-8:1990 standard. Unreinforced and fibre-reinforced cylindrical clay samples with a diameter of 38 mm and height of 76 mm were prepared at the same dry unit weight of 17.8 kN/m^3 and their equivalent moisture content on the dry side of the compaction curve (refer to **Figure 1**; see solid points). Soil samples were saturated with a B Skempton ratio of at least 0.97 using steps of back pressure and cell pressure and subsequently consolidated at initial effective consolidation stresses of 50 kPa, 100 kPa and 200 kPa, respectively to simulate the medium to relatively high in-situ effective stress ranges and consequently sheared at axial strain rate of 0.13%/min. There are a few studies investigating the effect of sample size on the unconfined compression strength (UCS) and shear strength of fibre-reinforced clays. Xiao et al., (2014) experienced a significant increase in the UCS of 7-day cured fibre-reinforced clay when the sample size increased from 50 mm to 100 mm. However, the change was minor when the sample size was changed from 100 mm to 150 mm. They also reported insignificant size effect on UCS of 14-day and 28-day cured fibre-reinforced samples. They also investigated the consolidated undrained and consolidated drained shear strength of fibre-reinforced clay and found that up to the consolidation stress of 110 kPa, the sample size does not affect the deviator stress of the fibre-reinforced clay significantly.

Nataraj and McManis (1997) also investigated the mechanical behaviour of fibre-reinforced clay using UCS test, direct shear test and CBR test. They reported an increase in UCS with the increase in sample size from 33 to 70 mm. However, they found the strength of 100 mm fibre-reinforced sample was slightly lower than that for 70 mm sample. Ang and Loehr (2003) also investigated the effect of sample size on the UCS of clays with diameter from 38 mm to 152 mm. They observed the highest UCS for 70 mm samples. They also concluded that sample size influences the UCS of the clay compacted at dry side of the optimum value significantly. Therefore, although there are no definite published results confirming the effect of sample size on the shear strength of clays in consolidated triaxial tests, a sample diameter to fibre length ratio of 8 is desirable as recommended by Xiao et al. (2014). In this study, due to the waste origin of the carpet fibres and their random size including fibre lengths from 2 mm to 20 mm and fibre diameters from 80 μm to 1,500 μm , the above criteria may have been met partially as there was no control on picking appropriate fibre lengths for sample preparation. On the other hand, smaller samples may not allow full mobilisation of the reinforcing role of fibres in fibre-reinforced soil resulting in underestimating the shear strength of fibre-reinforced clay (Ang and Loehr 2003).

4. Results and Discussions

The contributing effect of fibre reinforcement on the shear strength behaviour of clay samples in terms of deviator stress ratio-mean effective stress ratio (q_{ratio}/p'_{ratio}), effective stress ratio (q/p') and deviator stress (q) versus axial strain was analysed and discussed in the following sections.

4.1. Effective stress ratio and deviator stress of fibre-reinforced clay

The stress-strain relationships during the consolidated undrained triaxial test were normalised and plotted for effective stress ratio (q/p') and deviator stress versus axial strain for both unreinforced and fibre-reinforced soil samples at different initial effective consolidation stresses of 50 kPa, 100 kPa and 200 kPa as shown in **Figures 2 and 3**. **Figure 2** shows that inclusion of GBF fibre enhanced the effective stress ratio and deviator stress of the host soil significantly. Based on the graphs shown in **Figure 2a**, fibre-reinforced soil with 1%, 3% and 5% GBF fibre content improved the effective stress ratio of the unreinforced soil at initial effective consolidation stress of 200 kPa by 17.6%, 53.5% and 70.6%, respectively (i.e., measured at an axial strain of 20%). Although the effective stress ratios of the fibre-reinforced soil with 3% and 5% GBF fibre contents were almost similar at all effective consolidation stresses, their deviator stress behaviour was markedly different. This is mainly due to a simultaneous increase in both deviator stress and mean effective stress with the increase in fibre content resulting in less growth in effective stress ratio with the increase in fibre content. The ratio of deviator stress of 5% fibre-reinforced soil to that of 3% fibre-reinforced soil at an axial strain of 20% measured for initial effective consolidation stress of 200 kPa was determined to be 2.43 for GBF fibre-reinforced soil. The inclusion of 1%, 3% and 5% GBF fibre improved the deviator stress of the soil by 4.0%, 35.3% and 229.4% for the test with initial effective consolidation stress of 200 kPa (i.e., measured at an axial strain of 20%).

ABF fibre-reinforced soils also demonstrated significant improvement in effective stress ratio and deviator stress over those of unreinforced soil. At an axial strain of 20%, ABF fibre-reinforced soil samples subjected to initial effective consolidation stress of 200 kPa, produced 20.0%, 32.4% and 37.5% effective stress ratio improvement with

inclusion of 1%, 3% and 5% fibre, respectively (see **Figure 3a**). The inclusion of 1%, 3% and 5% ABF fibre, also improved the deviator stress of the soil by 16.7%, 38.4% and 129.3% at initial effective consolidation stress of 200 kPa (i.e., measured at an axial strain of 20%, **Figure 3b**). Fibre-reinforced soil samples with 3% fibre showed slightly higher effective stress ratio at initial effective consolidation stress of 50 kPa than that of 5% fibre-reinforced soil samples (See **Figures 2a and 3a**). However, with an increase in initial effective consolidation stress to 100 kPa and 200 kPa, the observed order was reversed. This observation for the behaviour of fibre-reinforced soil is consistent with results previously reported by Freilich and Zornberg (2010) as they observed an increase in effectiveness of fibres on the shear strength of the soil with the increase in the effective confining pressure. At higher initial effective consolidation stresses prior to the shearing stage, due to increase in confining pressure and hence improved interaction between soil particles and fibres, the fibres were increasingly stretched. Therefore, upon initiating the shear stage, the fibres contribute better to distributing the applied shear stresses into a wider area. However, at lower initial effective consolidation stresses, the fibres may not interact effectively with soil grains and hence may slip in shear. Hence at relatively low confining stresses, the fibres may not effectively confine soil grains nor add surplus strength to the reinforced soil. Therefore, an increase in the fibre content at a low initial effective consolidation stress may have an adverse effect on the strength of the reinforced soil without necessary soil grain harnessing effect.

Figures 2 and 3 also demonstrate that inclusion of fibres resulted in turning the plastic stress-strain behaviour of the unreinforced soil to a strain hardening behaviour. The shear strength behaviour of a soil is partly dependent on its initial moisture content and dry unit weight (Lamb and Whitman 1979). Reduction in the dry unit weight and increase in the moisture content of a soil mass subjected to shear stresses results in a rapid shear failure (Newcomb and Birgisson 1999). Although the moisture contents of the prepared soil samples were different and increased with fibre content, the shear strength ratio of the fibre-reinforced soil was superior to that of the unreinforced soil. The observed stress-strain response indicated that the contribution of the fibres to improve the shear strength of the soil samples prepared at an identical dry unit weight and different moisture contents, compensated for the loss of shear strength due to an increase in moisture content of the fibre-reinforced soil samples.

Repeatability and reliability of the shear strength test results of the fibre-reinforced soil are paramount for acquiring an accurate mechanical behaviour, deeper understanding and successful modelling of the fibre-reinforced clay behaviour. Although, a consistent and careful control was undertaken during the sample preparation phase to ensure uniform distribution of fibres within the clay sample, to confirm the reliability of results three tests repeated on the fibre-reinforced clay samples with 5% ABF fibre content at initial consolidation stresses of 50, 100 and 200 kPa, respectively. **Figure 4** compares the original and the repeat test results and shows a good repeatability of the results. In this study, the deviator stress ratio and mean effective stress ratio are defined as the ratio of the deviator and mean effective stress of the fibre-reinforced soil to that of the unreinforced soil, respectively:

$$\text{Deviator stress ratio } (q_{ratio}) = \frac{q_{re}}{q_{un}} \quad (\text{Eq.1})$$

$$\text{Mean effective stress ratio } (p'_{ratio}) = \frac{p'_{re}}{p'_{un}} \quad (\text{Eq.2})$$

where; q is the deviator stress ($\sigma'_1 - \sigma'_3$), p' is the mean effective stress ($(1/3)(\sigma'_1 + 2\sigma'_3)$) and $\sigma'_{1,3}$ are the major and

minor principal effective stresses

Note: re: reinforced, un: unreinforced

Figure 5 presents the relationships between q_{ratio} and p'_{ratio} of the fibre-reinforced soil samples. Illustrated data in this figure are related to the data of q_{ratio} , and p'_{ratio} of the fibre-reinforced soil samples subjected to initial effective consolidation stresses of 50 kPa, 100 kPa and 200 kPa and calculated at axial strains of 5%, 10%, 15% and 20%, respectively. **Figure 5** also shows that q_{ratio} changed rather linearly with p'_{ratio} at all fibre contents for both fibre types and the deviator stress ratio and mean effective stress ratio of the fibre-reinforced soil increased with fibre content. Assuming q_{ratio} a linear function of p'_{ratio} , we can write:

$$q_{ratio} = z \times p'_{ratio} + w \quad (Eq.3)$$

Equation 3 shows that a linear relationship existed between the deviator stress ratio and mean effective stress ratio of the fibre-reinforced soil. However, this equation did not specifically elaborate on the above relationship as a function of axial strain during triaxial compression test, fibre content and initial consolidation stress of the soil sample. Therefore, it is required to develop models to correlate the effective stress ratio and deviator stress of the fibre-reinforced soil to the axial strain, fibre content and initial consolidation stress of the clay sample during the triaxial compression test.

4.2. Predicting the effective stress ratio and deviator stress of fibre-reinforced soil

Duncan-Chang model (i.e., hyperbolic stress-strain theory, 1970) is an incremental nonlinear stress-dependent model that explains the nonlinearity, stress-dependent and inelastic behavioural feature of cohesive and cohesionless soils with a simple form. Horpibulsuk and Miura (2001) and Horpibulsuk and Rachan (2004) used a modified form of the Duncan-Chang hyperbolic model to capture the undrained and drained behaviour of uncemented and cement stabilised clays. The modified hyperbolic model can exhibit strain softening behaviour following the destruction of the sample at peak and also the strain hardening behaviour. Therefore, in this study, the modified hyperbolic model proposed by Horpibulsuk and Miura (2001) was used to characterise the nonlinear stress-strain behaviour of the fibre-reinforced clay.

In order to consider the nonlinear behaviour (i.e., strain hardening/softening) of the effective stress ratio and deviator stress of the fibre-reinforced clay, the variation of the effective stress ratio and deviator stress of the fibre-reinforced soil with the axial strain in terms of modified hyperbolic relation takes the following forms:

$$\frac{q}{p'} = \frac{\varepsilon}{a + b\varepsilon^n} \quad \text{a, b and n are the modified hyperbolic model parameters for effective stress ratio (Eq.4)}$$

$$q = \frac{\varepsilon}{g + h\varepsilon^t} \quad \text{g, h and t are the modified hyperbolic model parameters for deviator stress (Eq.5)}$$

The parametric study of the influence of model parameters on the evolution of effective stress ratio ($\frac{q}{p'}$) and deviator stress (q) are shown in **Figures 6** and **7**, respectively. **Figure 6** shows that a controlled the value of the initial tangent to the $q/p' - \varepsilon$ behaviour while b accounted for the residual value and n was responsible for the slope of the post peak drop of the $q/p' - \varepsilon$ curve.

The effective stress ratio and deviator stress data of the consolidated undrained triaxial tests on both unreinforced and fibre-reinforced soil samples were used to determine the coefficients of the modified hyperbolic model using a nonlinear regression analysis. **Figures 8 and 9** show the calculated coefficients for both unreinforced and fibre-reinforced soil samples tested at different initial effective consolidation stresses. The calculated hyperbolic model parameters for the stress-strain behaviour of the fibre-reinforced samples with different fibre contents and subjected to different initial effective consolidation stresses showed a nonlinear trend for both ABF and GBF fibres. Therefore, to develop a set of meaningful correlations between calculated coefficients and the fibre content, the parameters were further normalised to the values of initial effective consolidation stress and fibre content. The following equations show the relationships between the normalised coefficients and the initially non-normalised coefficients used in the modified hyperbolic model. **Figures 10 and 11** depict the relationships between the normalised parameters and the fibre content.

$$a^* = \log\left(\frac{a}{100\sigma'_c}\right)(1 + 100f) = k_{1a} \times f + k_{2a} \quad (\text{Eq.6})$$

$$b^* = \log\left(\frac{b}{100}\right)(1 + 100f) = k_{1b} \times f + k_{2b} \quad (\text{Eq.7})$$

$$n^* = \text{Exp}(-n)(1 + 100f) = k_{1n} \times f + k_{2n} \quad (\text{Eq.8})$$

$$g^* = \log\left(\frac{\sigma'_c g^2}{100}\right)(1 + 100f) = k_{1g} \times f + k_{2g} \quad (\text{Eq.9})$$

$$h^* = \log\left(\frac{\sigma'_c h^2}{100}\right)(1 + 100f) = k_{1h} \times f + k_{2h} \quad (\text{Eq.10})$$

$$t^* = \text{Log}(100t)(1 + 100f) = k_{1t} \times f + k_{2t} \quad (\text{Eq.11})$$

where; σ'_c stands for the initial effective consolidation stress, f stands for the fibre content and

$k_{1a,g}, k_{2a,g}, k_{1b,h}, k_{2b,h}, k_{1n,t}, k_{2n,t}$ are the coefficients of the linear equations (see **Figures 10 and 11**).

Therefore, the original coefficients of the modified hyperbolic model can be expressed based on the fibre content, initial effective consolidation stress and the linear equations presented in **Figures 10 and 11** using **equations 12 to 17**.

$$a = \sigma'_c 10^{(2 + \frac{k_{1a} \times f + k_{2a}}{1 + 100f})} \quad (\text{Eq.12})$$

$$b = 10^{(2 + \frac{k_{1b} \times f + k_{2b}}{1 + 100f})} \quad (\text{Eq.13})$$

$$n = -\ln\left(\frac{k_{1n} \times f + k_{2n}}{1 + 100f}\right) \quad (\text{Eq.14})$$

$$g = \sqrt{\frac{1}{\sigma'_c} 10^{(2 + \frac{k_{1g} \times f + k_{2g}}{1 + 100f})}} \quad (\text{Eq.15})$$

$$h = \sqrt{\frac{1}{\sigma'_c} 10^{(2 + \frac{k_{1h} \times f + k_{2h}}{1 + 100f})}} \quad (\text{Eq.16})$$

$$t = 10^{(-2 + \frac{k_{1t} \times f + k_{2t}}{1 + 100f})} \quad (\text{Eq.17})$$

Combining **equations 4 and 5** with **equations 12 to 17** results in the following equations for predicting the effective shear stress ratio and deviator stress of the fibre-reinforced clay:

$$\left(\frac{q}{p'}\right)_{re} = \frac{0.01 \times \varepsilon}{\sigma'_c \times 10^{\frac{k_1 a \times f + k_2 a}{1+100f}} + 10^{\left(\frac{k_1 b \times f + k_2 b}{1+100f}\right) \varepsilon - \ln\left(\frac{k_1 n \times f + k_2 n}{1+100f}\right)}} \quad (\text{Eq.18})$$

$$q_{re} = \frac{0.01 \times \varepsilon}{\sqrt{\frac{1}{\sigma'_c} 10^{\frac{k_1 g \times f + k_2 g}{1+100f}} + \varepsilon^{10^{\left(-2 + \frac{k_1 t \times f + k_2 t}{1+100f}\right)}}} \sqrt{\frac{1}{\sigma'_c} 10^{\frac{k_1 h \times f + k_2 h}{1+100f}}}} \quad (\text{Eq.19})$$

Equations 18 and 19 can also be rewritten for unreinforced soil (i.e., $f = 0$):

$$\left(\frac{q}{p'}\right)_{un} = \frac{0.01 \times \varepsilon}{\sigma'_c \times 10^{k_2 a + 10^{k_2 b \times \varepsilon - \ln(k_2 n)}}} \quad (\text{Eq.20})$$

$$q_{re} = \frac{0.01 \times \varepsilon}{\sqrt{\frac{1}{\sigma'_c} 10^{k_2 g + \varepsilon^{10^{(k_2 t - 2)}}} \sqrt{\frac{1}{\sigma'_c} 10^{k_2 h}}}} \quad (\text{Eq.21})$$

Figure12 compares the predicted data using the developed regression model for the relationships between effective stress ratio and axial strain of the unreinforced and fibre-reinforced soil samples studied in this research.

4.3. Proposed method to predict the stress ratio of fibre-reinforced clays

In this study, the modified hyperbolic model was used to predict the effective stress ratio and deviator stress of the fibre-reinforced clay for practical application. The model parameters can be calculated using the following steps:

- 1) Use **equations 4 and 5** to fit the test data of unreinforced and fibre-reinforced soil samples using nonlinear regression analysis and determine a, b and n or g, h and t.
- 2) Use **equations 6 to 11** to calculate the normalised parameters a^* , b^* and n^* or g^* , h^* and t^* .
- 3) Draw the best fit line through the graphs of normalised parameters (calculated in step 2) versus fibre content to calculate $k_{1a,g}$, $k_{2a,g}$, $k_{1b,h}$, $k_{2b,h}$, $k_{1n,t}$ and $k_{2n,t}$.
- 4) Use **equations 18 and 19** to predict the effective stress ratio and deviator stress of the fibre-reinforced clay, respectively.

The model calibration phase as explained above aims to capture the inherent properties of the soil and fibres into the equation in form of model parameters. Therefore, once the model is calibrated based on a particular clay type and a particular fibre type, it can predict the effective shear stress ratio and deviator stress of the clay at different axial strains during the triaxial compression test. The model parameters can be adequately estimated using a minimum of 2 tests on an unreinforced soil (at two different initial effective consolidation stresses) and two tests on fibre-reinforced clay (with a fibre content at two different initial effective consolidation stresses). A medium range fibre content is recommended for calibration stage. To increase the accuracy of the model it is recommended to use the triaxial test data of three unreinforced soil samples tested at different effective consolidation stresses.

4.4. Validation of the model

The proposed model was validated by comparing its predictions with some of the published experimental data available in the literature. The stress-strain data of the chosen research works were extracted by digitising the reported graphs.

Wu et al. (2014) carried out a series of undrained triaxial tests on fibre-reinforced silty clay samples with 0.5%, 1% and 1.5% sisal fibres. They reported a gradual increase in deviator stress of fibre-reinforced soil with an increase in fibre content. However, the rate of deviator stress improvement was declined beyond 1% fibre content. **Figure 13** shows the predicted data using the model introduced in this study. The model parameters were calculated using experimental data of the unreinforced and 1% fibre-reinforced samples tested at consolidation stresses of 100 kPa and 400 kPa, respectively. The developed model in this study could predict the experimental results at 200 kPa consolidation stress for 0.5%, 1% and 1.5% fibre-reinforced clay with 0.5% to 5% underestimation.

Babu and Chouksey (2010) also carried out a series of undrained tests on randomly distributed fibre-reinforced clay samples with 0.5%, 1% and 2% coir fibres. The results indicated that the fibre-reinforced soil gained a higher strength than unreinforced soil with the increase in fibre content to the studied limit of 2% fibre content. They also developed an analytical model based on Cam Clay model to predict the shear strength of fibre-reinforced soil. Although their model fitted well with the experimental results, they did not validate their model with published data. **Figure 14** shows the experimental results reported in their article and the predicted data using the proposed model in this study. The model parameters were acquired from triaxial test data carried out on unreinforced and 1% fibre-reinforced soil at consolidation stresses of 50 and 150 kPa, respectively. According to **Figure 14**, the ratios of the effective stress ratio of 0.5%, 1% and 2% coir fibre-reinforced clay predicted by the developed model in this study to that of the experimental results at consolidations stress of 100 kPa at 12% axial strain were 1.03, 0.99 and 0.95, respectively.

Ozkul and Baykal (2007) reported an increase in drained and undrained deviator stress of saturated silty clay reinforced with 10% short tyre buffing fibres. They also determined a limiting confining pressure of 200-300 kPa beyond which the presence of rubber fibres reduced the shear strength of the soil. The undrained experimental data reported by Ozkul and Baykal (2007) was used to validate the model developed in this study. Therefore, the model parameters were calculated using the test data of unreinforced soil at consolidation stresses of 100 kPa and 300 kPa in addition to the single test data of fibre-reinforced soil at consolidation stress of 300 kPa. **Figure 15** shows the experimental data and predicted deviator stress curves. The ratios of the deviator stresses of 10% rubber fibre-reinforced clay predicted by the developed model in this study to that of the experimental results at consolidation stresses of 100 kPa, 200 kPa and 300 kPa at 12% axial strain were 1.04, 0.97 and 0.99, respectively.

In another study, Nguyen and Fatahi (2016) reported the mechanical behaviour of fibre-reinforced cemented clay with polypropylene fibres using a series of consolidated undrained triaxial tests. They also developed a constitutive model called C3F based on Modified Cam Clay (MCC) model to predict the shear strength of fibre-reinforced clays with and without cementation. Their model could predict the shear strength of the fibre-reinforced cemented clay in a good agreement with the experimental results. **Figure 16** shows the undrained experimental results on fibre-reinforced clay samples stabilised with 15% cemented, predicted results using C3F model and also the predicted test data using the method introduced in this study. The model parameters were acquired using data of unreinforced and 0.5% fibre-reinforced soil tested at effective consolidation stresses of 400 kPa and 800 kPa, respectively. According to **Figure 16**, at consolidation stress of 200 kPa and 12% axial strain the developed model in this study

overestimated the deviator stress of 0.3% and 0.5% fibre-reinforced soil by 4% and 15% respectively and the C3F model underestimated both by 4%. However, at 800 kPa consolidation stress and 12% axial strain, the developed model in this study and C3F model overestimated the deviator stress of 0.3% and 0.5% fibre-reinforced soil both by the same values of 16% and 10%, respectively.

Khatri et al. (2016) also carried out a series of undrained triaxial tests on fibre-reinforced clay with 0.4% to 1.6% coir fibre. They reported that the shear strength of fibre-reinforced clay was improved with the increase in fibre content and developed a successful hyperbolic model to predict their own data. However, they did not correlate the model parameters with fibre content or consolidation stress and their model was not validated against available data in the literature. **Figure 17** compares the experimental data and those predicted by the developed model in this study. The model parameters were calculated using experimental data of unreinforced and 0.8% fibre-reinforced soil at consolidation stresses of 77.48 kPa and 313.92 kPa, respectively. The developed model in this study underestimated the effective stress ratio of the 0.4%, 0.8% and 1.6% fibre-reinforced soil at consolidation stress of 77.48 kPa and 12% axial strain by 10%, 10% and 3%, respectively. However, at consolidation stress of 313.92 kPa and 12% axial strain, the effective stress ratio of 0.4%, 0.8% and 1.6% fibre-reinforced soil was overestimated by 18%, 1% and 5%, respectively.

Table 3 demonstrates a comparison of experimental and predicted results of above-studied research works. The developed nonlinear regression model based on the modified hyperbolic model and the proposed technique to acquire the model parameters in this study could capture the experimental stress-strain results reasonably well considering the less effort to calculate the model parameters compared to using constitutive models.

The **Supplemental Material** for this article explains the technique to calculate the model parameters for the modified hyperbolic model based on the triaxial test results reported by **Wu et al. (2014)**.

5. Conclusions

In this research, the shear strength behaviour of a clay reinforced with two types of carpet waste fibre was investigated by conducting a set of consolidated undrained triaxial shear tests on fibre-reinforced samples with 1%, 3% and 5% fibre contents. The fibre-reinforced soils exhibited significant variation in the Proctor compaction curve to that of the unreinforced soil. Therefore, to eliminate the effect of initial unit weight on the stress-strain results, all samples were prepared at an identical dry unit weight (i.e., 17.8 kN/m³) and their respective moisture contents based on the standard Proctor compaction curves for the unreinforced and fibre-reinforced soils.

Fibre reinforcement using waste carpet fibres improved the stress-strain behaviour of the clay significantly and the contribution of the fibres to increase the effective stress ratio and deviator stress of the soil increased with fibre content. At higher initial effective consolidation stresses prior to the shearing stage, fibres stretch increasingly and therefore, contribute better to distribute the disturbing shear stresses into a wider area upon initiating the shear stage. However, at lower initial effective consolidation stresses, fibres cannot stretch effectively and may slip during the shear. Hence, fibres may not confine soil grains and add surplus strength to the reinforced soil. Therefore, increase in fibre content at a low initial effective consolidation stress may have an insignificant effect on the shear strength of

the fibre-reinforced soil without necessary soil grain harnessing effect. Increase in fibre content results in changing the stress-strain behaviour of the unreinforced soil sample to a strain hardening behaviour. This research indicated that up to 5% carpet waste fibre could be optimally used for improving the shear strength behaviour of clay and hence introduces carpet waste fibres as sustainable soil reinforcing materials to improve the shear strength of weak soils.

Two nonlinear regression models were developed based on the modified hyperbolic model to predict the effective stress ratio and deviator stress of the fibre-reinforced clay. The model parameters can be determined from the triaxial test results on unreinforced and a fibre-reinforced soil sample at two different consolidation stresses. The model can predict the stress-strain curve of the fibre-reinforced clay with knowing the initial effective consolidation stress and the fibre content. The model was verified with the available data in the literature and predictions by the model agreed reasonably well with the published experimental data. The proposed model is relatively simple compared to other developed regression models and constitutive models reported in the literature in that it eliminates the requirement for advanced soil testing and knowledge of fibre properties. This model can be used as a tool to predict the shear strength of fibre-reinforced clay in geotechnical engineering practice with limited knowledge of the soil properties and less number of testing.

Acknowledgements

The authors wish to express their gratitude to Envirolink Northwest (United Kingdom) for funding part of this project, Carpet Recycling UK and Milliken Industries for supplying the fibres. The fourth author is grateful to a financial support from Suranaree University of Technology and the Thailand Research Fund under the TRF Senior Research Scholar program Grant No. RTA5980005.

References

- Ahmad, F., Bateni, F., Azmi, M. (2010). "Performance evaluation of silty sand reinforced with fibres." *J. of Geotex. and Geomem.*, 28(1), 93-99.
- Al-Akhras, N. M., Attom, M. F., Al-Akhras, K. M., Malkawi, A. I. H. (2008). "Influence of fibers on swelling properties of clayey soil." *Geosynthetics Int. J.*, 15(4), 304-309.
- Ang, E. C., Loehr, J. E. (2003). "Specimen size effects for fiber-reinforced silty clay in unconfined compression" *Geotechnical Testing Journal* 26(2), 1-10.
- Anggraini, V., Asadi, A., Farzadnia, N., Jahangirian, H., Huat, B. B. K. (2016). "Effects of coir fibres modified with $\text{Ca}(\text{OH})_2$ and $\text{Mg}(\text{OH})_2$ nanoparticles on mechanical properties of lime-treated marine clay." *Geosynthetics Int. J.*, 23(3), 206-218.
- Babu, G. L. S., and Chouksey, S. K. (2010). "Model for analysis of fiber-reinforced clayey soil." *Geomech. Geoeng.*, 5(4), 277-285.
- Babu, G. L.S., Vasudevan, A. K. (2008). "Strength and stiffness response of coir fiber-reinforced tropical soil." *J. of Mat. in Civil Eng.*, 20(9), 571-577.
- Botero, E., Ossa, A., Sherwell, G., and Ovando-Shelley, E. (2015). "Stress-strain behavior of a silty soil reinforced with polyethylene terephthalate (PET)." *J. of Geotex. and Geomem.*, 43(4), 363-369.
- British Standards Institution. 1990. BS 1377: Part 8: 1990 British Standard Methods of test for Soils for civil engineering purposes-Part 8. Shear strength tests (effective stress). British Standards Institution. United Kingdom.
- Chen, C. W., and Loehr, J. E. (2009). "Undrained and drained triaxial tests of fiberreinforced sand." *Geosynthetics in Civil and Environmental Engineering*, 114-120.
- Chen, C. W. (2007). "A constitutive model for fiber-reinforced soil." Ph.D. thesis, Univ. of Missouri, Colombia, USA.
- Casagrande, M.D.T., Coop, M.R., Consoli, N. (2006). "Behavior of a Fiber-Reinforced Bentonite at Large Shear Displacements." *J. of Geotech. Geoenviron. Eng.*, 132(11), 1505-1508.
- Consoli, N.C., Casagrande, M.D.T., Coop, M.R. (2007). "Performance of fibre-reinforced sand at large shear strains." *Geotechnique*, 57(9), 751-756.
- Diambra A., Ibraim E., Wood M., Russell A. (2010). "Fiber reinforced sands: experiments and modelling." *J. of Geotex. and Geomem.*, 28, 238-50.
- Diambra, A., Russell, A. R., Ibraim, E. and Muir Wood, D. (2007). "Determination of fibre orientation distribution in reinforced sand." *Geotechnique*, 57(7), 623-628.
- Diambra, A., Ibraim, E. (2014). "Modelling of fibre cohesive soil mixtures." *Acta Geotech.*, 9, 1029-1043.

- Duncan, J.M. and Chang, C.Y. (1970). "Nonlinear analysis of stress and strain in soils." *J. of Soil Mechanics & Foundations Div.*, 96(5), 1629-1653.
- Ekinci, A., and Ferreira, P. (2012). "The undrained mechanical behavior of fiber reinforced heavily over-consolidated clay", TC 211 - International symposium on Recent Research, Advances & Execution Aspects of Ground Improvement works, Brussels, Belgium, 53-62.
- Falorca, I. M.C.F.G., Pinto, M. I.M. and Ferreira, G. L. M. (2006). "Residual shear strength of sandy clay reinforced with short polypropylene fibers randomly oriented." In: *Proceeding of 8th int. conf. on geosynt. (8ICG)*, Yokohama, 4, 1663-1666.
- Fatahi, B., Fatahi, B., Le, T. M., and Khabbaz, H. (2013a). "Small-strain properties of soft clay treated with fibre and cement." *Geosynthetics Int.*, 20(4), 286-300.
- Fatahi, B., Khabbaz, H. & Fatahi, B. (2012). "Mechanical characteristics of soft clay treated with fibre and cement." *Geosynthetics Int. J.*, 19(3), 252-262.
- Fatahi, B., Le, T. M., Fatahi, B., and Khabbaz, H. (2013b). "Shrinkage properties of soft clay treated with cement and geofibers." *Geotech. Geol. Eng. J.*, 31(5), 1421-1435.
- Freilich, B.J., Li, C. and Zornberg, J.G. (2010). "Effective shear strength of fiber-reinforced clays." In *9th International Conference on Geosynthetics, Brazil, 1997-2000*.
- Ghiassian, H., Poorebrahim, G. and Gray, D. (2004). "Soil Reinforcement with Recycled Carpet Wastes.", *Waste Management & Research J.*, 22, 108-114.
- Gray, D.H. and Ohashi, H. (1983). "Mechanics of Fiber Reinforced in Sand." *Journal of Geotec. and Geoenv. Eng.*, 109(3), 335-353.
- Hamidi, A., Hooresfand, M. (2013). "Effect of fiber reinforcement on triaxial shear behavior of cement treated sand." *J. of Geotex. and Geomem.*, 36,1-9.
- Horpibulsuk, S., and Miura, N. (2001). "Modified hyperbolic stress-strain response: uncemented and cement stabilized clays", Report of the Faculty of Science and Engineering, Saga University, Japan, 30(1), 39-47.
- Horpibulsuk, S. and Rachan, R. (2004), "Modified hyperbolic model for capturing undrained shear behavior." *Lowland Technology International*, 6(2), 11-20.
- Jamsawang, P., Voottipruex, P. and Horpibulsuk, S. (2015), "Flexural strength characteristics of compacted-cement-polypropylene fiber-sand" *J. of Mat. in Civil Eng.*, 27(9), 04014243(1-9).
- Khatri, V. N., Dutta, R. K., Venkataraman, G., & Shrivastava, R. (2016). "Shear Strength Behaviour of Clay Reinforced with Treated Coir Fibres." *Periodica Polytechnica. Civil Eng.*, 60(2), 135-143.
- Lambe, T. W., and Whitman, R. V. (1979), "Soil Mechanics," 2d ed., John Wiley & Sons, Inc., New York, USA.
- Maher, M.H., Gray, D.H. (1990). "Static response of sands reinforced with randomly distributed fibers." *J. of*

- 453 *Geotech. Eng.*, 116(11), 1661-1677.
- 454 Maliakal, T., and Thiyyakkandi, S. (2013), "Influence of randomly distributed coir fibers on shear strength of clay."
 455 *Geotechnical and Geological Engineering*, 31(2), 425-433.
- 456 Michalowski, R.L. (2008). "Limit analysis with anisotropic fibre-reinforced soil." *Geotechnique*, 58(6), 489-502.
- 457 Michalowski R L, Zhao A. (1996). "Failure of fiber-reinforced granular soils." *J. of Geotec. Eng.*, 122(3), 226-234.
- 458 Miranda Pino, L. and Baudet, B. (2015). "The effect of the particle size distribution on the mechanics of fibre-
 459 reinforced sands under one-dimensional compression." *J. of Geotex. and Geomem.* 43 (3), 250-258.
- 460 Mirzababaei, M., Miraftab, M., Mohamed, M. and McMahon, P. (2013a). "Impact of waste carpet fibres on swelling
 461 properties of compacted clays." *J. of Geotech. and Geolo. Eng.*, 31(1), 173-182.
- 462 Mirzababaei, M., Miraftab, M., Mohamed, M. and McMahon, P. (2013b). "Unconfined Compression Strength of
 463 Reinforced Clays with Carpet Waste Fibers." *J. of Geotech. Geoenviron. Eng.*, 139(3), 483-493.
- 464 Mirzababaei, M., Arulrajah, A., Horpibulsuk, S., and Aldava, M. (2017a). "Shear strength of a fibre-reinforced clay
 465 at large shear displacement when subjected to different stress histories." *Geotextiles and Geomembranes*,
 466 <https://doi.org/10.1016/j.geotexmem.2017.06.002>.
- 467 Mirzababaei, M., Mohamed, M., and Miraftab, M. (2017b). "Analysis of strip footings on fiber-reinforced slopes
 468 with the aid of particle image velocimetry." *Journal of Materials in Civil Engineering*, 29(4),
 469 [https://doi.org/10.1061/\(ASCE\)MT.1943-5533.0001758](https://doi.org/10.1061/(ASCE)MT.1943-5533.0001758).
- 470 Murray, J. J.; Frost, J. D. and Wang, Y. (2000). "Behavior of a sandy silt reinforced with discontinuous recycled
 471 fiber inclusions." *Transportation Research Record Journal*, 1714, 9-17.
- 472 Nataraj, M.S. and McManis, K.L. (1997). "Strength and Deformation Properties of Soils Reinforced With Fibrillated
 473 Fibers." *Geosynthetics Int. J.*, 4(1), 65-79.
- 474 Newcomb, D. E., Birgisson, B. (1999). "Measuring In Situ Mechanical Properties of Pavement Subgrade Soils."
 475 National Cooperative Highway Research Program, Project 20-5FYA 1996, Washington, USA.
- 476 Nguyen, L., Fatahi, B. (2016). "Behaviour of clay treated with cement & fibre while capturing cementation
 477 degradation and fibre failure – C3F Model" *Int. J. of Plasticity*, 81, 168-195.
- 478 Özkul, Z.H. and Baykal, G. (2007). "Shear behavior of compacted rubber fiber-clay composite in drained and
 479 undrained loading." *J. of geotechnical and Geoenvironmental engineering*, 133(7), 767-781.
- 480 Ranjan, G., Vasan, R. M., Charan, H. D. (1996). "Probabilistic analysis of randomly distributed fiber-reinforced
 481 soil." *J. of Geotech. Eng.*, 122(6), 419-426.
- 482 Sadeghi, M., Beigi, F. H. (2014). "Dynamic behavior of reinforced clayey sand under cyclic loading." *J. of*
 483 *Geotex. and Geomem.*, 42(5), 564-572.

- Shukla, S. K., Shivakugan, N., Singh, A. K. (2010). "Analytical model for fiber-reinforced granular soil under high confining stress." *J. of Mat. in Civil Eng.*, 22(9), 935-942.
- Waldron, L. J. (1977). "The shear resistance of root permeated homogeneous and stratified soil." *Soil Science Society of America Proceedings*, 41, 843-849.
- Wu, Y., Li, Y. and Niu, B. (2014). "Assessment of the mechanical properties of sisal fiber-reinforced silty clay using triaxial shear tests." *The Scientific World Journal*, 2014, 436231.
- Özkul, Z.H. and Baykal, G. (2007). "Shear behavior of compacted rubber fiber-clay composite in drained and undrained loading." *J. of geotechnical and Geoenvironmental engineering*, 133(7), 767-781.
- Xiao, H.W., Yannick, N.C.H., Lee, F.H., Zhang, M.H., Ahmad B.S. (2014). "Size effect study on fibre-reinforced cement-treated clay" *Proceedings of the International Symposium on Geomechanics and Geotechnics: From Micro to Macro*, Cambridge, U.K., 1351 -1356.
- Zornberg, J. G. (2002). "Discrete framework for limit equilibrium analysis of fibre-reinforced soil." *Geotechnique*, 52(8), 593-604.

List of Figures:

- Figure 1.** Standard Proctor compaction curves of fibre-reinforced clays
- Figure 2.** Effective stress ratio a) and deviatoric stress b) behaviours of GBF fibre-reinforced clay
- Figure 3.** Effective stress ratio a) and deviatoric stress b) behaviours of ABF fibre-reinforced clay
- Figure 4.** Results of repeated test on 5% ABF fibre-reinforced clay
- Figure 5.** The relationship between deviator stress change ratio and mean effective stress change ratio of fibre-reinforced clays
- Figure 6.** Parametric study of the modified hyperbolic model parameters on the effective stress ratio of the soil: the effect of a) parameter 'a' b) parameter 'b' c) parameter 'n' on the modified hyperbolic function
- Figure 7.** Parametric study of the modified hyperbolic model parameters on the deviatoric stress of the soil: the effect of a) parameter 'g' b) parameter 'h' c) parameter 't' on the modified hyperbolic function
- Figure 8.** Modified hyperbolic model parameters for $q/p' - \varepsilon$ behaviour of the fibre-reinforced soil samples
- Figure 9.** Modified hyperbolic model parameters for $q - \varepsilon$ behaviour of the fibre-reinforced soil samples
- Figure 10.** Normalised modified hyperbolic model parameters for $q/p' - \varepsilon$ behaviour of the fibre-reinforced soil samples: a,b,c) ABF fibre-reinforced soils d,e,f) GBF fibre-reinforced soils
- Figure 11.** Normalised modified hyperbolic model parameters for $q - \varepsilon$ behaviour of the fibre-reinforced soil samples: a,b,c) ABF fibre-reinforced soils d,e,f) GBF fibre-reinforced soils
- Figure 12.** Experimental and predicted data for effective stress ratio-axial strain response of: (a) GBF fibre-reinforced soil (b) ABF fibre-reinforced soil
- Figure 13.** Experimental and predicted data for shear strength response of fibre-reinforced soil (Wu et al., 2014)
- Figure 14.** Experimental and predicted data for shear strength response of fibre-reinforced soil (Babu and Chouksey, 2010)

Figure 15. Experimental and predicted data for shear strength response of fibre-reinforced soil (Ozkul and Baykal, 2007)

Figure 16. Experimental and predicted data for shear strength response of fibre-reinforced soil (Nguyen and Fatahi 2016)

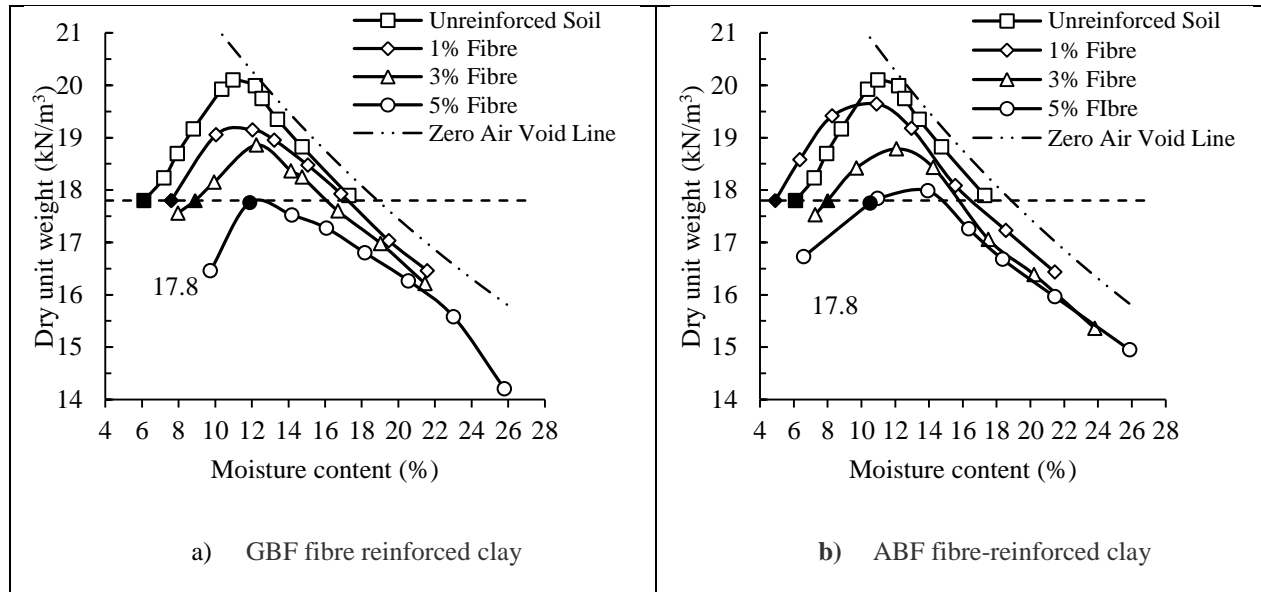
Figure 17. Experimental and predicted data for shear strength response of fibre-reinforced soil (Khatri et al., 2016

List of Tables:

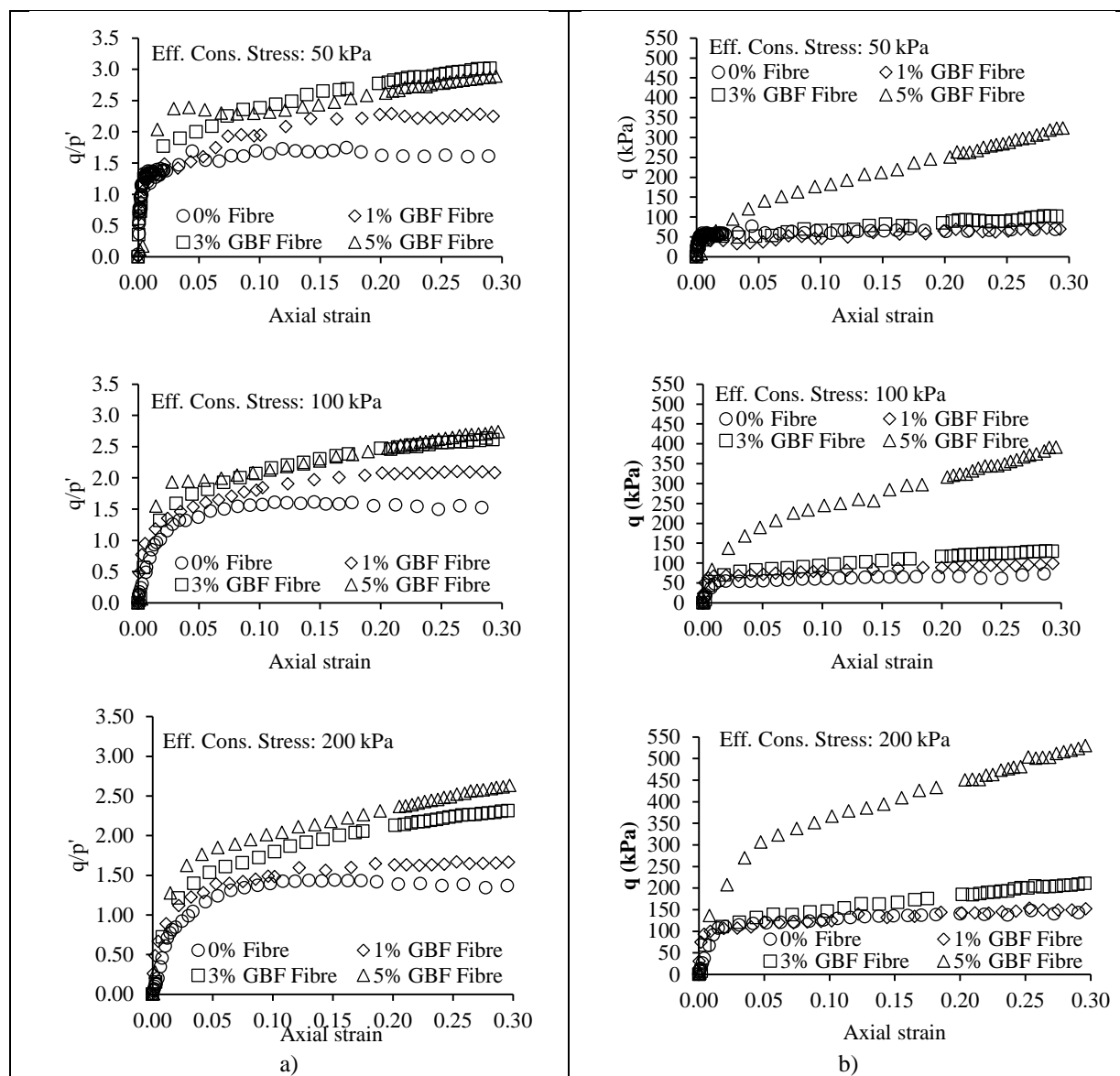
Table 1. Soil Properties

Table 2. Properties of carpet waste fibres

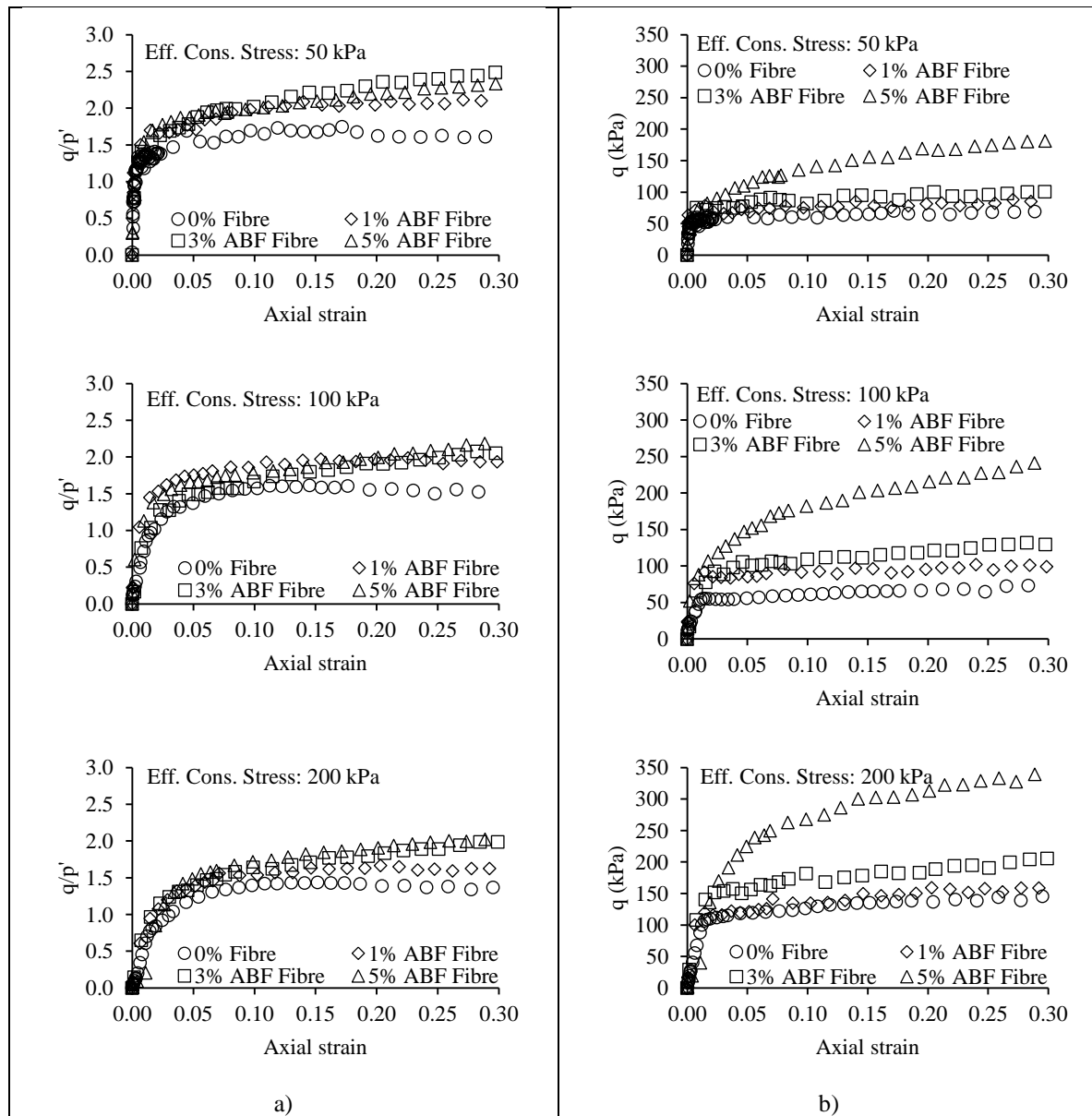
Table 3. Comparison of experimental and predicted shear strength results



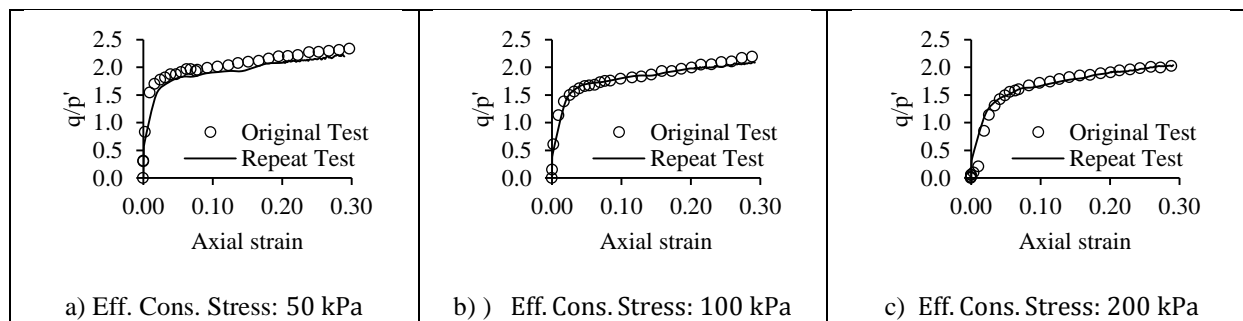
530 Figure 1. Standard Proctor compaction curves of fibre-reinforced clays



531 Figure 2. Effective stress ratio a) and deviatoric stress b) behaviours of GBF fibre-reinforced clay



532 Figure 3. Effective stress ratio a) and deviatoric stress b) behaviours of ABF fibre-reinforced clay



533 Figure 4. Results of repeated tests on 5% ABF fibre-reinforced clay

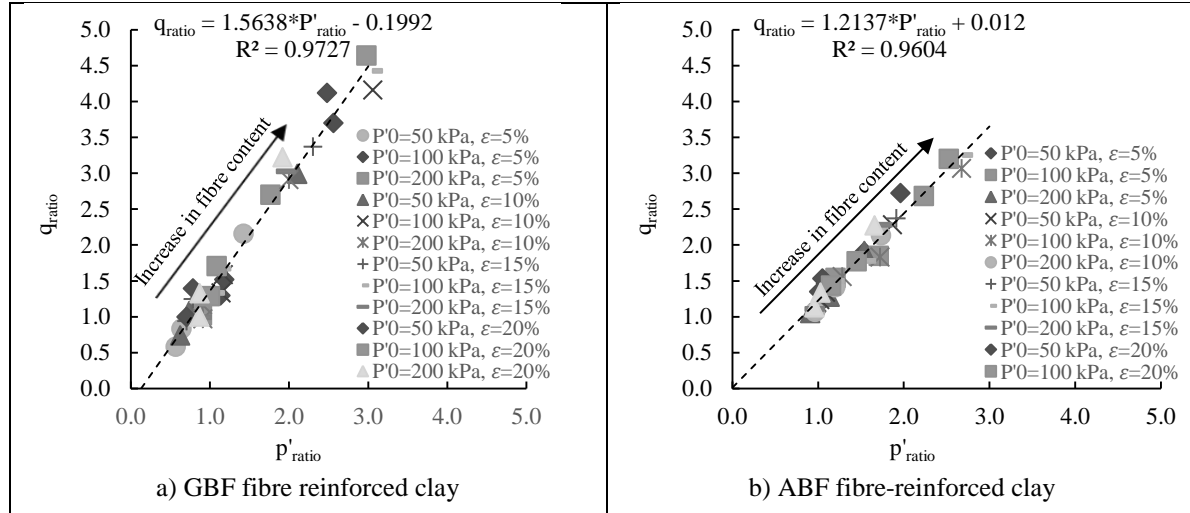


Figure 5. The relationship between deviator stress change ratio and mean effective stress change ratio of fibre-reinforced clays

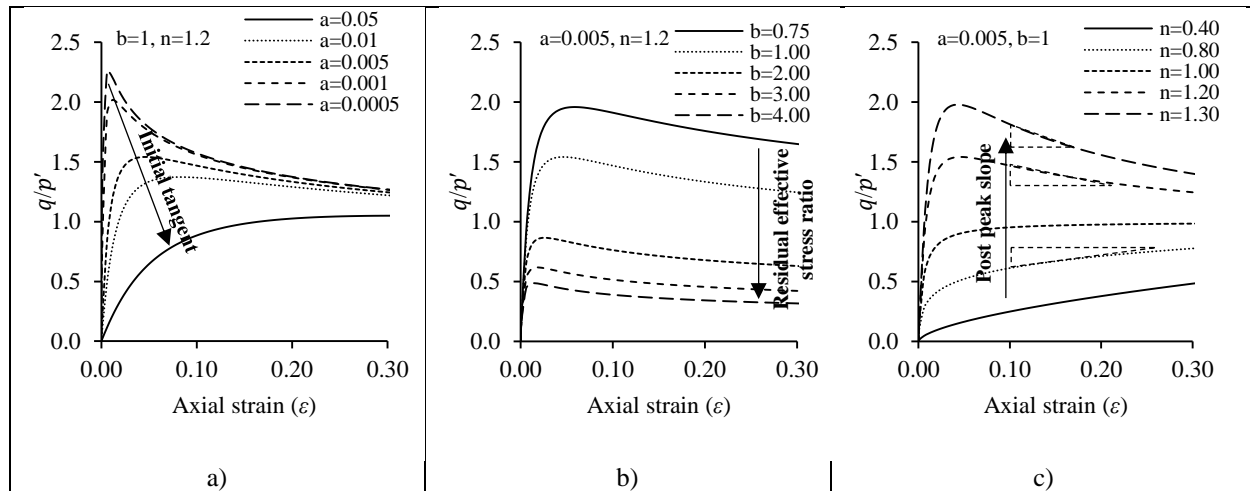


Figure 6. Parametric study of the modified hyperbolic model parameters on the effective stress ratio of the soil: the effect of a) parameter 'a' b) parameter 'b' c) parameter 'n' on the modified hyperbolic function

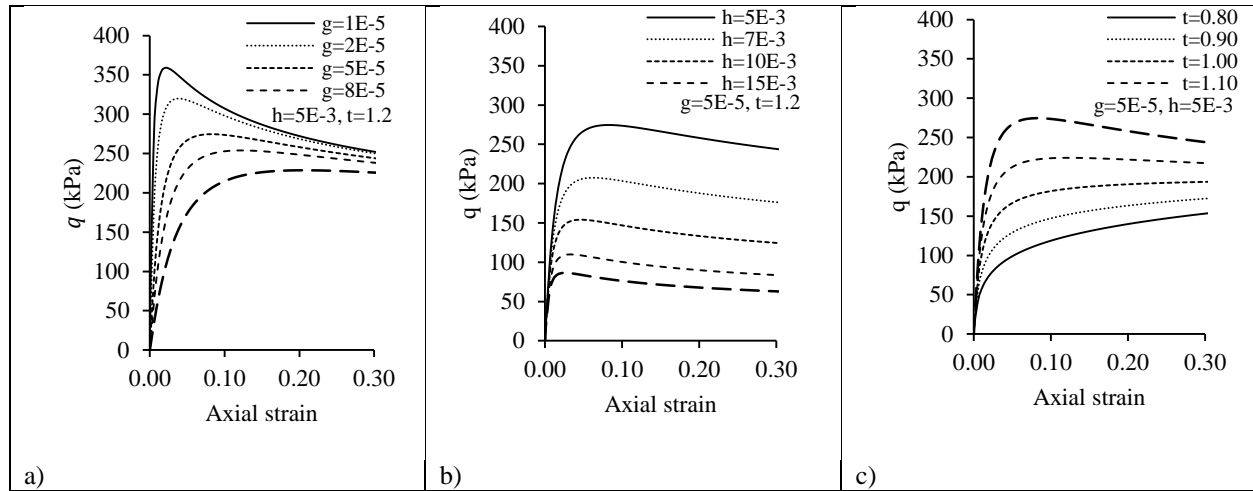
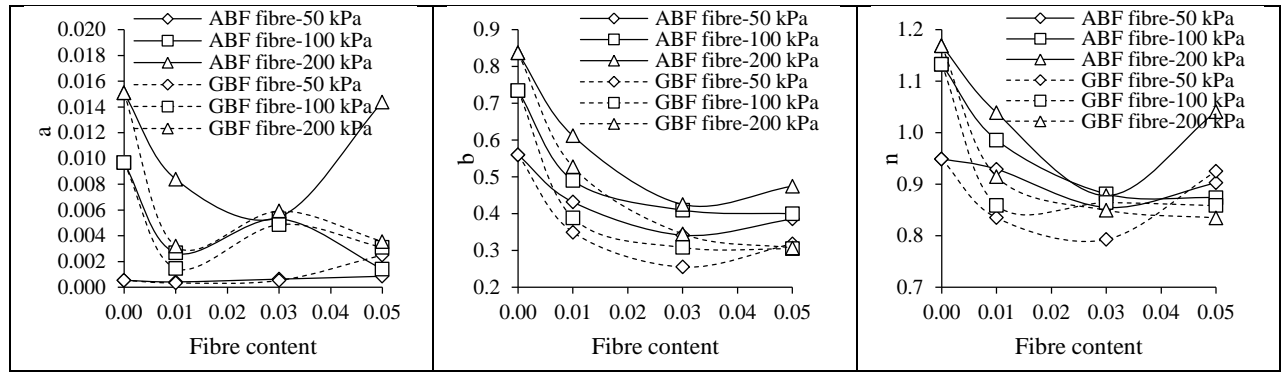
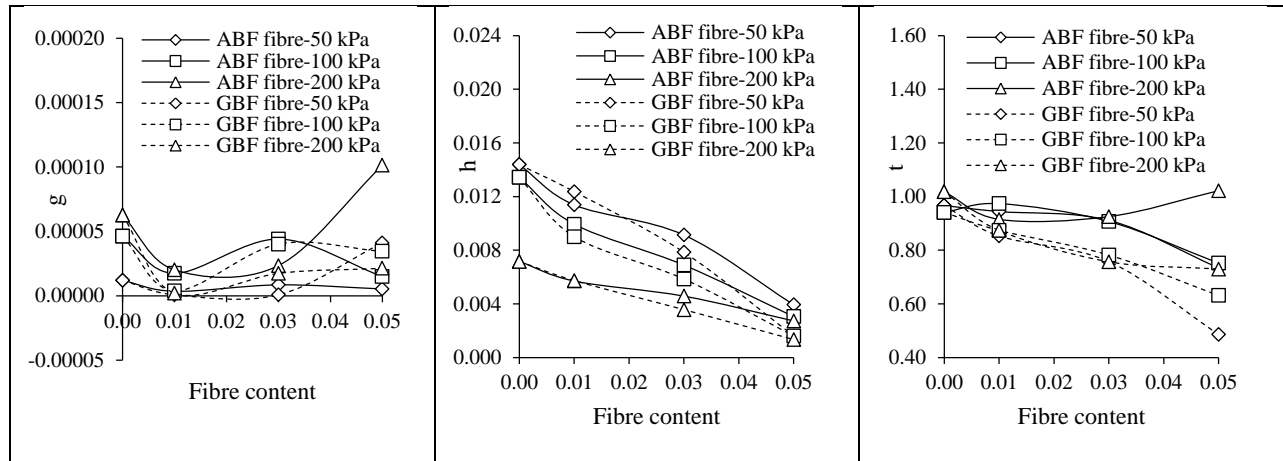


Figure 7. Parametric study of the modified hyperbolic model parameters on the deviatoric stress of the soil: the effect of a) parameter 'g' b) parameter 'h' c) parameter 't' on the modified hyperbolic function



540 Figure 8. Modified hyperbolic model parameters for $q/p' - \varepsilon$ behaviour of the fibre-reinforced soil samples



541 Figure 9. Modified hyperbolic model parameters for $q - \varepsilon$ behaviour of the fibre-reinforced soil sample

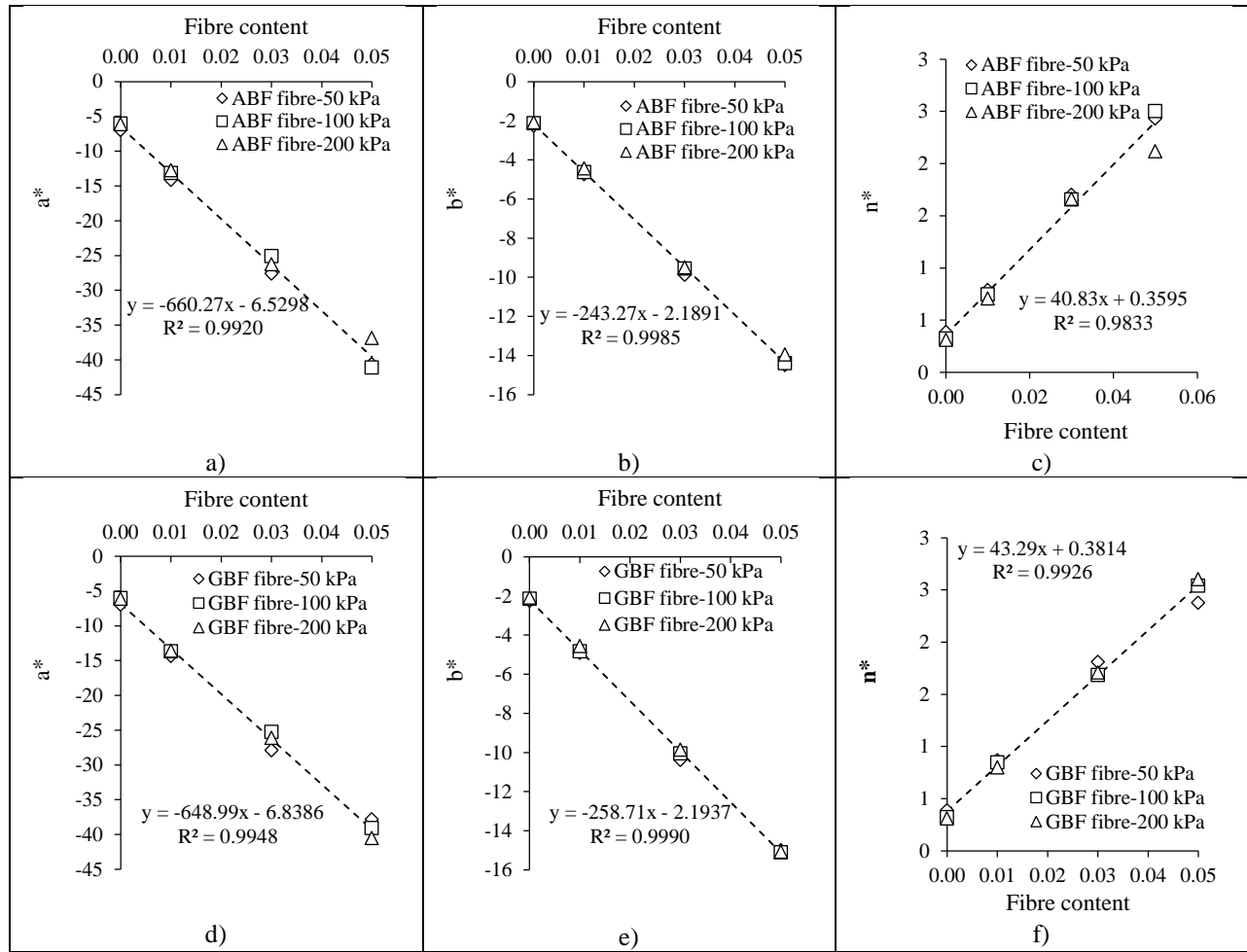


Figure 10. Normalised modified hyperbolic model parameters for $q/p' - \varepsilon$ behaviour of the fibre-reinforced soil samples: a,b,c) ABF fibre-reinforced soils d,e,f) GBF fibre-reinforced soils

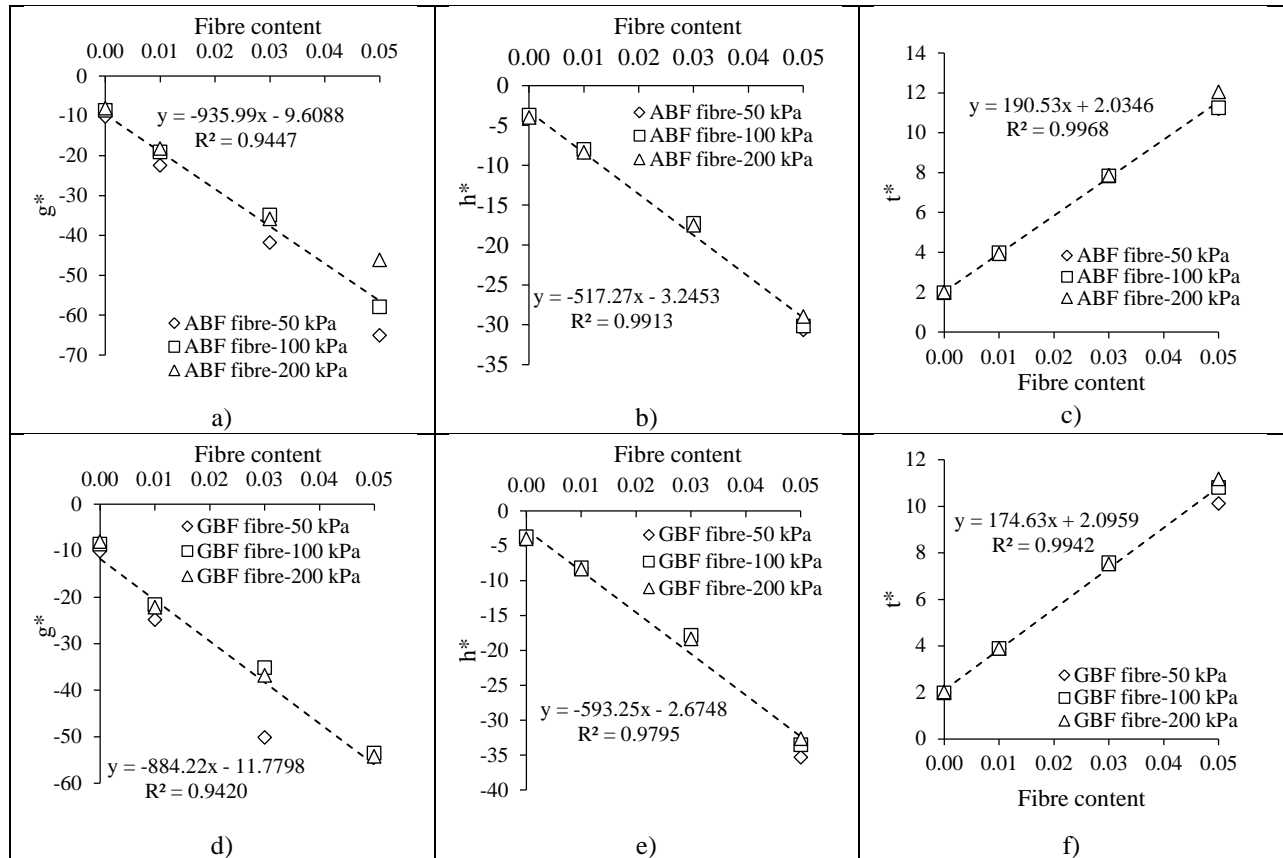


Figure 11. Normalised modified hyperbolic model parameters for $q - \epsilon$ behaviour of the fibre-reinforced soil samples: a,b,c) ABF fibre-reinforced soils d,e,f) GBF fibre-reinforced soils

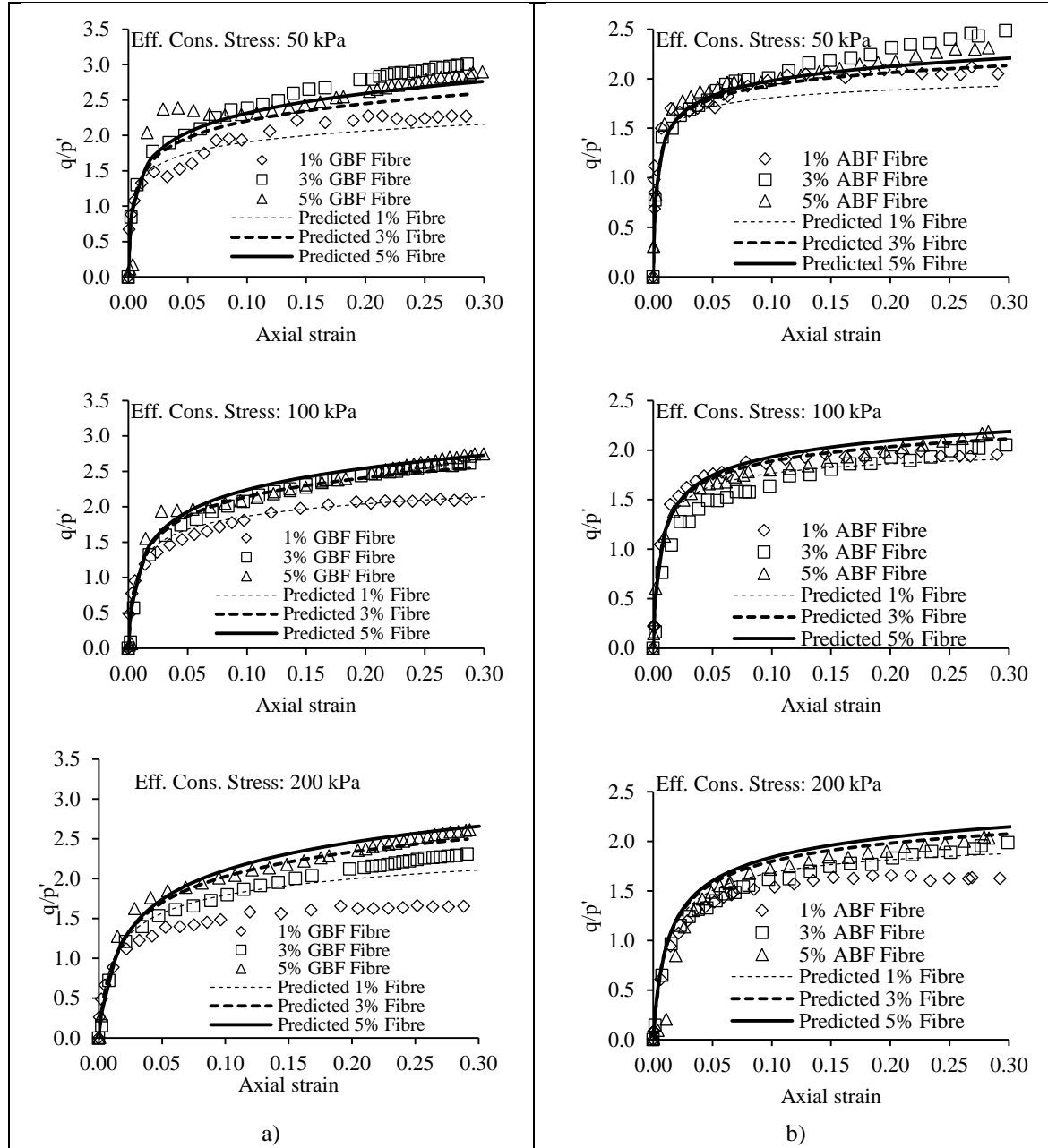
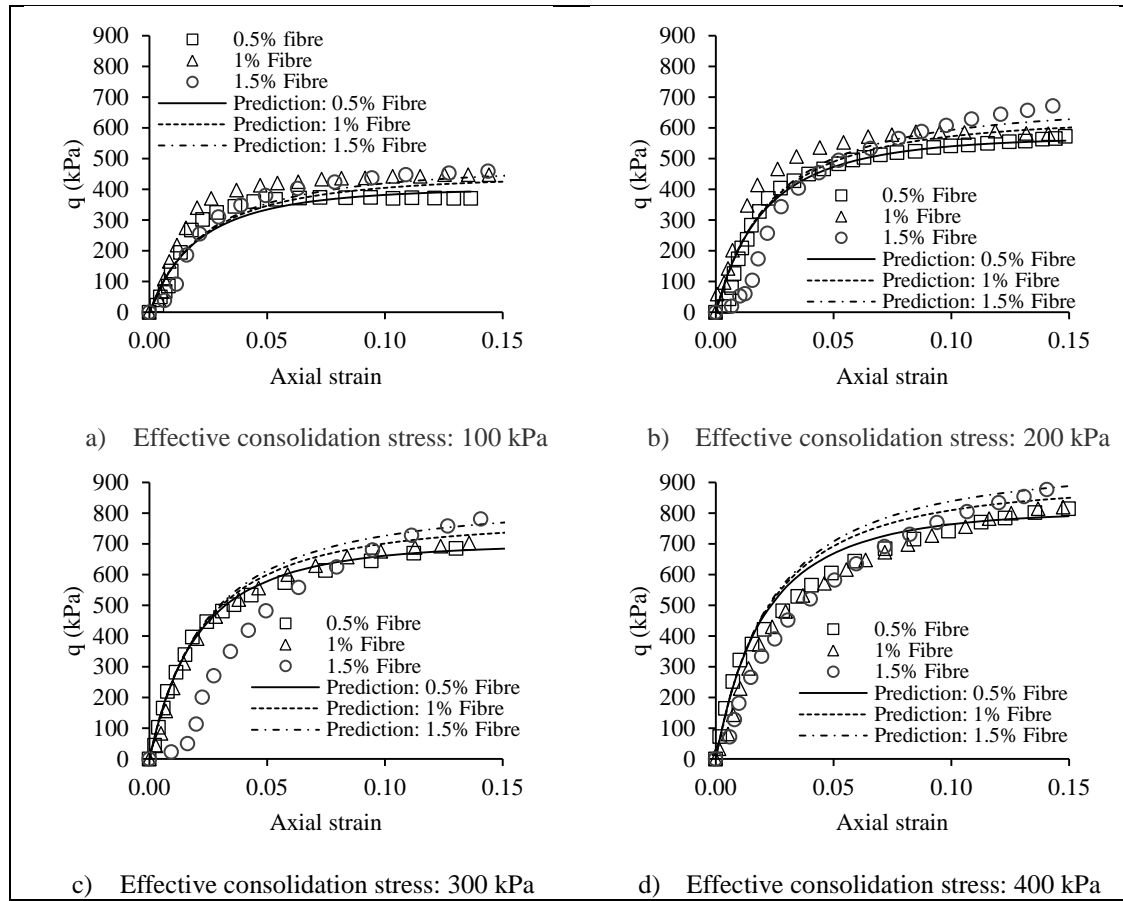


Figure 12. Experimental and predicted data for effective stress ratio-axial strain response of:

a) GBF fibre-reinforced soil b) ABF fibre-reinforced soil



548 Figure 13. Experimental and predicted data for shear strength response of fibre-reinforced soil (Wu et al. 2014)

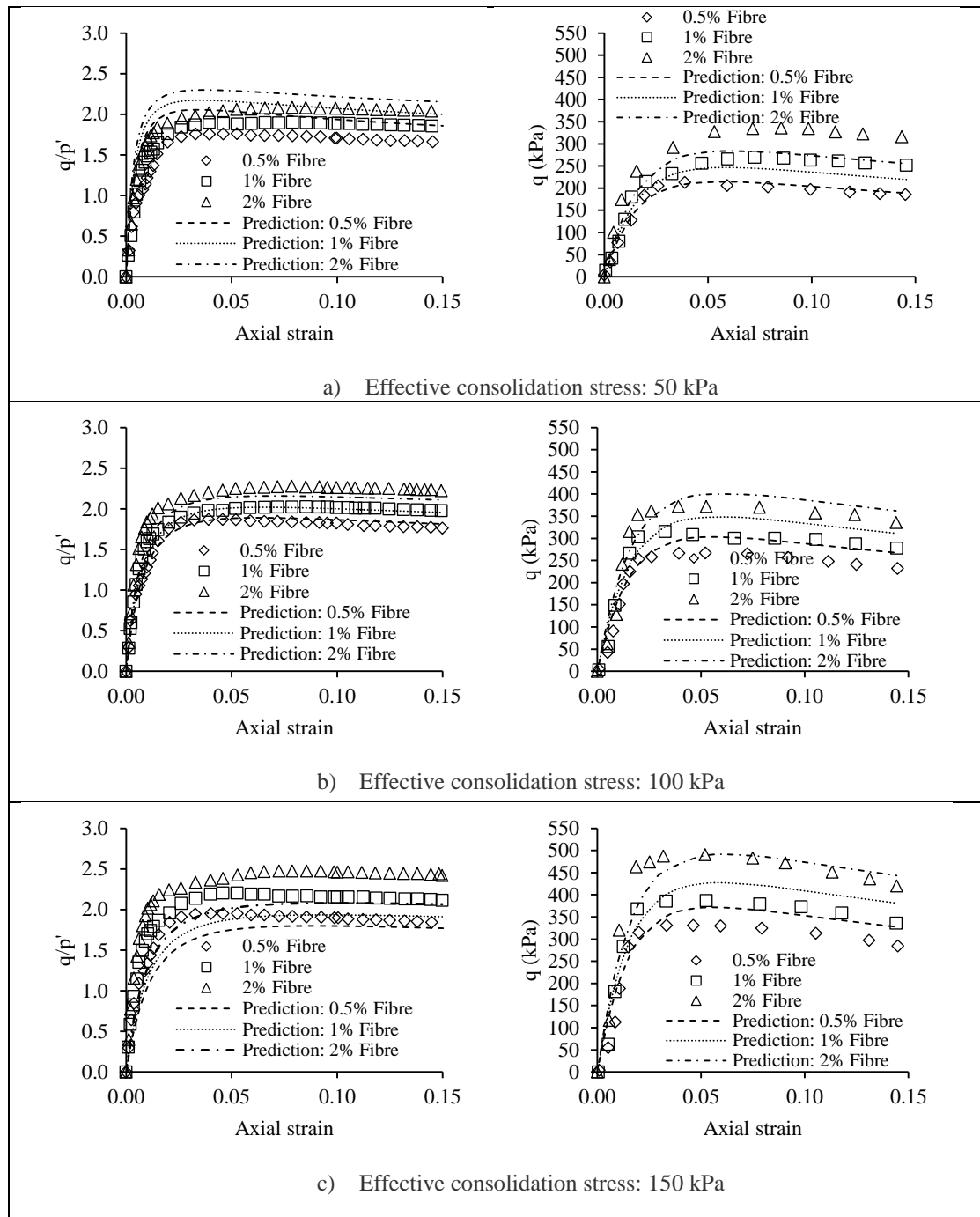


Figure 14. Experimental and predicted data for shear strength response of fibre-reinforced soil (Babu and Chouksey 2010)

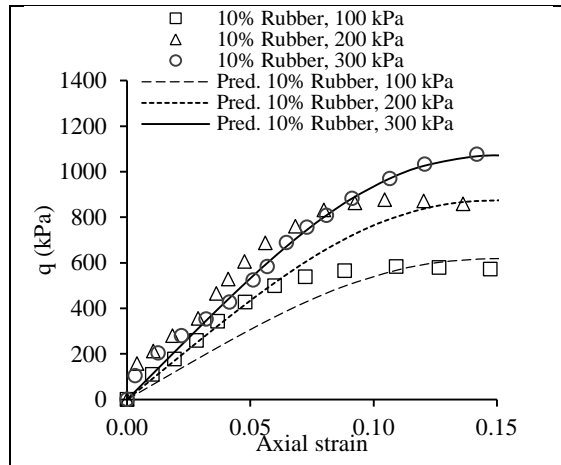


Figure 15. Experimental and predicted data for shear strength response of fibre-reinforced soil (Ozkul and Baykal 2007)

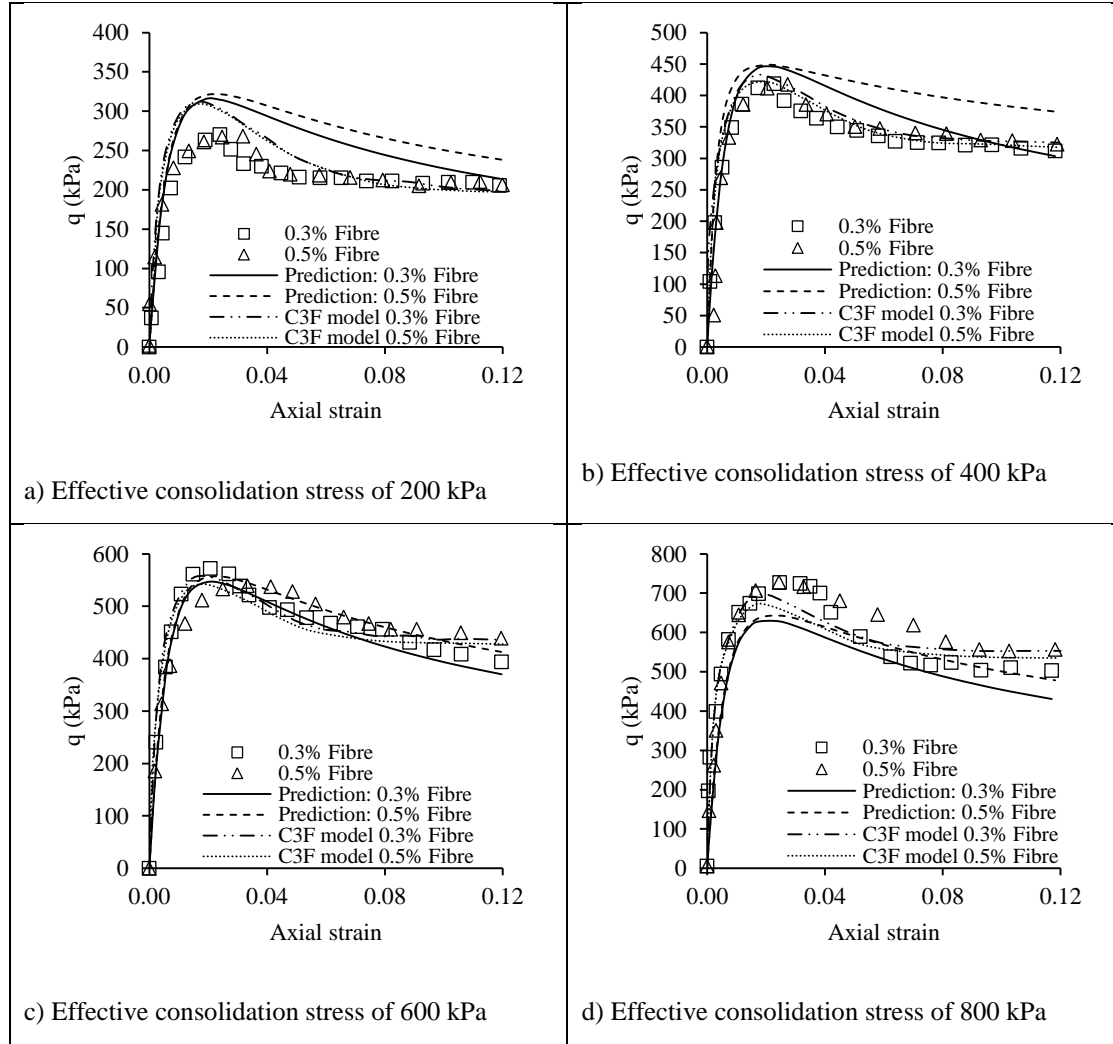


Figure 16. Experimental and predicted data for shear strength response of fibre-reinforced soil (Nguyen and Fatahi 2016)

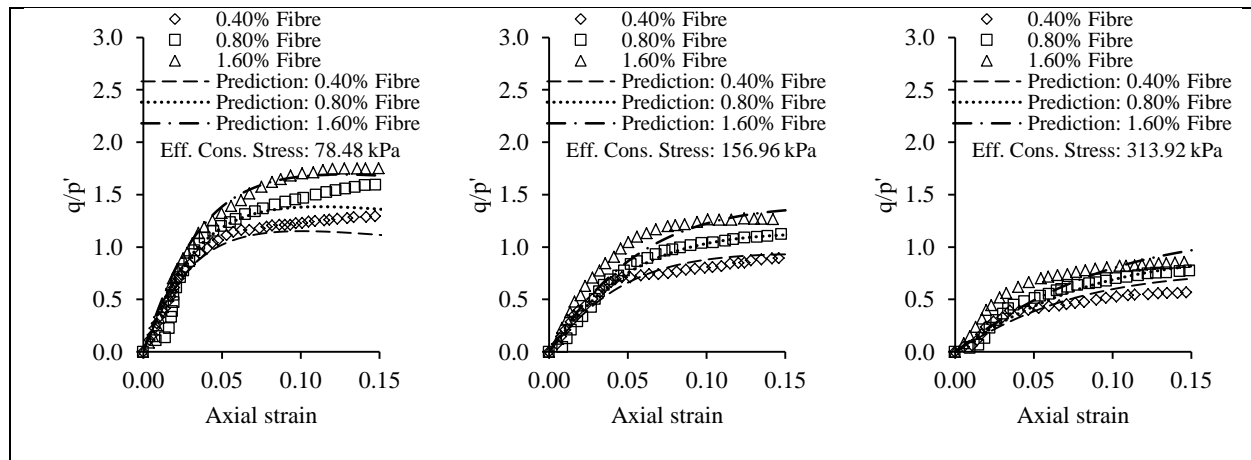


Figure 17. Experimental and predicted data for shear strength response of fibre-reinforced soil (Khatri et al. 2016)

556

Table 1. Soil Properties

Unified soil classification	CL
Specific gravity	2.68
Gravel (%)	1.42
Sand (%)	42.80
Fine content (%)	55.78
Liquid limit (%)	29.00
Plastic Limit (%)	12.00
Plasticity index (%)	17.00
Maximum dry unit weight (kN/m ³)	20.10
Optimum moisture content (%)	11.00
Swelling pressure (kPa)	76.20

557

Table 2. Properties of carpet waste fibres

Composition		Specific Gravity*	Water Absorption* (%)	Composition (%)	Specific Tensile Modulus* (GPa/gram/cm ³)
GBF fibre	Polypropylene	0.90	0.0	60	0.27~0.44
	Styrene-Butadiene Rubber (SBR)	0.99	-	20	-
	Nylon	1.14	4.1-4.5	15	0.40~0.70
	Wool	1.32	13-15	5	0.27~0.40
ABF fibre	Nylon	1.14	4.1-4.5	100	0.40~0.70

*Recommended by the manufacturer

558

559

Table 3. Comparison of experimental and predicted shear strength results

Test data	$\frac{(\frac{q}{p'})_{predicted}}{(\frac{q}{p'})_{experiment}}$	$\frac{q_{predicted}}{q_{experiment}}$	
$\varepsilon = 14.5\%, f = 0.5\%, \sigma'_c = 50 \text{ kPa}$	1.12	1.02	Babu and Chouksey (2010)
$\varepsilon = 14.3\%, f = 1\%, \sigma'_c = 50 \text{ kPa}$	1.08	0.87	
$\varepsilon = 14.3\%, f = 2\%, \sigma'_c = 50 \text{ kPa}$	1.06	0.81	
$\varepsilon = 14.4\%, f = 0.5\%, \sigma'_c = 100 \text{ kPa}$	1.03	1.16	
$\varepsilon = 14.4\%, f = 1\%, \sigma'_c = 100 \text{ kPa}$	0.99	1.12	
$\varepsilon = 14.4\%, f = 2\%, \sigma'_c = 100 \text{ kPa}$	0.94	1.08	
$\varepsilon = 14.5\%, f = 0.5\%, \sigma'_c = 150 \text{ kPa}$	0.96	1.15	
$\varepsilon = 14.5\%, f = 1\%, \sigma'_c = 150 \text{ kPa}$	0.90	1.14	
$\varepsilon = 14.4\%, f = 2\%, \sigma'_c = 150 \text{ kPa}$	0.85	1.05	
$\varepsilon = 13.6\%, f = 0.5\%, \sigma'_c = 100 \text{ kPa}$	-	1.06	Wu et al. (2014)
$\varepsilon = 14.4\%, f = 1\%, \sigma'_c = 100 \text{ kPa}$	-	0.94	
$\varepsilon = 14.4\%, f = 1.5\%, \sigma'_c = 100 \text{ kPa}$	-	0.96	
$\varepsilon = 14.1\%, f = 0.5\%, \sigma'_c = 200 \text{ kPa}$	-	0.98	
$\varepsilon = 14.1\%, f = 1\%, \sigma'_c = 200 \text{ kPa}$	-	1.03	
$\varepsilon = 14.3\%, f = 1.5\%, \sigma'_c = 200 \text{ kPa}$	-	0.93	
$\varepsilon = 14.1\%, f = 1.5\%, \sigma'_c = 300 \text{ kPa}$	-	0.98	
$\varepsilon = 14.1\%, f = 1.5\%, \sigma'_c = 400 \text{ kPa}$	-	1.01	
$\varepsilon = 14.7\%, f = 10\%, \sigma'_c = 100 \text{ kPa}$	-	1.08	Ozkul and Bykal (2007)
$\varepsilon = 13.6\%, f = 10\%, \sigma'_c = 200 \text{ kPa}$	-	1.01	
$\varepsilon = 14.2\%, f = 10\%, \sigma'_c = 300 \text{ kPa}$	-	0.99	
$\varepsilon = 10.5\%, f = 0.3\%, \sigma'_c = 600 \text{ kPa}$	-	0.94	Nguyen and Fatahi (2016)
$\varepsilon = 10.5\%, f = 0.5\%, \sigma'_c = 600 \text{ kPa}$	-	0.95	
$\varepsilon = 10.5\%, f = 0.3\%, \sigma'_c = 800 \text{ kPa}$	-	0.88	
$\varepsilon = 10.5\%, f = 0.5\%, \sigma'_c = 800 \text{ kPa}$	-	0.90	
$\varepsilon = 14.2\%, f = 0.4\%, \sigma'_c = 78.48 \text{ kPa}$	0.88	-	Khatri et al. (2016)
$\varepsilon = 14.1\%, f = 1.6\%, \sigma'_c = 78.48 \text{ kPa}$	0.97	-	
$\varepsilon = 14.1\%, f = 0.4\%, \sigma'_c = 156.96 \text{ kPa}$	1.04	-	
$\varepsilon = 14.2\%, f = 1.6\%, \sigma'_c = 156.96 \text{ kPa}$	1.06	-	
$\varepsilon = 14.1\%, f = 0.4\%, \sigma'_c = 313.92 \text{ kPa}$	1.22	-	
$\varepsilon = 14.5\%, f = 1.6\%, \sigma'_c = 313.92 \text{ kPa}$	1.12	-	

SUPPLEMENTAL MATERIAL

In this example, the model parameters of the introduced modified hyperbolic model are calculated for experimental data reported by Wu et al. (2014). A nonlinear regression analysis using the modified hyperbolic function (Eq. 5) was carried out on the stress-strain data of the unreinforced and 1% fibre-reinforced soil tested at effective consolidation stresses of 100 kPa and 400 kPa, respectively. **Figure S1** shows the yielded modified hyperbolic and normalised modified hyperbolic regression model parameters (**Equations 9 to 11**) for calibrating the model. In order to determine the linear coefficients ($k_{1a,g}$, $k_{2a,g}$, $k_{1b,h}$, $k_{2b,h}$, $k_{1n,t}$ and $k_{2n,t}$), draw a graph of normalised modified hyperbolic model parameters versus fibre content and find the best fit line (See **Figure S2**). Then use **equations 15 to 17** to calculate the modified hyperbolic model parameters (g , h and t). Finally, use **equation 5 or 19** to predict the deviator stress of the fibre-reinforced clay.

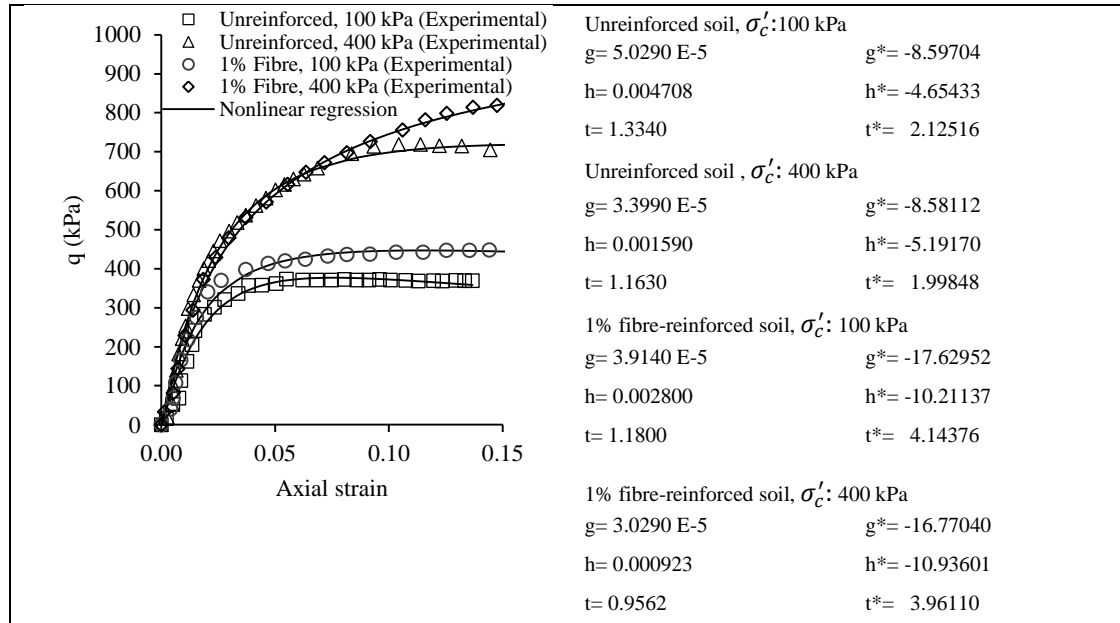
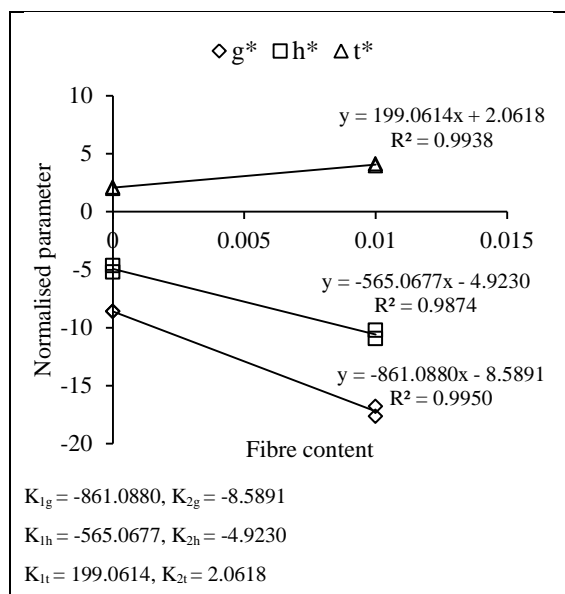


Figure S1. Experimental data and modified hyperbolic nonlinear regression analysis of deviator stress of unreinforced and fibre-reinforced soil (Wu et al., 2014)



577 Figure S2. Relationship between normalised modified hyperbolic parameters and fibre content